

Bioequivalence Assessment for Locally Acting Drugs: A Framework for Feasible and Efficient Evaluation

LUCA INSOLIA¹⁻³, YANYUAN MA⁴,
YOUNES BOULAGUIEM⁵ & STÉPHANE GUERRIER^{1-3,*}

¹School of Pharmaceutical Sciences, University of Geneva, Geneva, Switzerland; ²Institute of Pharmaceutical Sciences of Western Switzerland, University of Geneva, Geneva, Switzerland; ³Department of Earth Sciences, University of Geneva, Geneva, Switzerland; ⁴Department of Statistics, The Pennsylvania State University, University Park, Pennsylvania, USA; ⁵Geneva School of Economics and Management, University of Geneva, Geneva, Switzerland.

Abstract

Equivalence testing plays a key role in several domains, such as the development of generic medical products, which are therapeutically equivalent to brand-name drugs but with reduced cost and increased accessibility. Promoting access to generics is a critical public health issue with substantial societal implications, but establishing equivalence is particularly challenging in multivariate settings. A notable example refers to locally acting drugs designed to exert their therapeutic effects at a localized area where they are administered rather than being absorbed into the bloodstream, where complex experimental protocols lead to reduced sample sizes and substantial experimental noise. Traditional approaches, such as the Two One-Sided Tests (TOST), cannot adequately tackle the complex multivariate nature of such data. In this work, we develop an adjustment for the TOST procedure by simultaneously correcting its significance level and equivalence margins to ensure control of the test size and increase its power. In large samples, this approach leads to an optimal adjustment for the univariate TOST procedure. In multivariate settings, where we show that an optimal adjustment does not exist, our proposal maintains equal marginal test sizes and overall size control while maximizing power in important cases. Through extensive simulation studies and a case study on multivariate bioequivalence assessment for two antifungal topical products, we demonstrate the superior performance of our method across various scenarios encountered in practice.

Keywords: composite hypothesis testing, equivalence test, finite-sample adjustments, locally acting drugs, two one-sided tests.

1 Introduction

Average equivalence testing aims at detecting whether an average effect of interest, such as the difference in two means, falls within a predetermined region of practical equivalence. Nowadays, there is an ever-increasing interest in equivalence testing problems, especially in multivariate contexts ([Pallmann and Jaki 2017](#)). These problems arise in many disciplines, such as psychology ([Lakens et al. 2018](#)), engineering ([Moore et al. 2022](#)), software development ([Dolado et al. 2014](#)), and social sciences ([Aggarwal et al. 2023](#)), to name a few. Equivalence testing plays a prominent role in the pharmaceutical sciences, where it is typically referred to as bioequivalence testing. Bioequivalence studies play a key role in developing generic drugs, which are therapeutically equivalent to brand-name drugs but with reduced cost and increased medication accessibility. Promoting the accessibility of generic medical products is an important public health concern with significant social and economic effects (see e.g., [Lukic et al. 2020](#), [Shin et al. 2020](#), [Miranda et al. 2022](#)). A key aspect of the approval process for generics involves demonstrating their therapeutic equivalence to well-investigated brand-name drugs (see e.g., [Patterson and Jones 2017](#)). As most administered drugs enter the bloodstream to reach their site of action, their assessment traditionally relies on comparing the active ingredient concentrations in the blood using pharmacokinetic parameters (e.g., the area under the blood concentration-time curve or the peak concentration). A test drug (such as a new generic drug) and a

reference drug (such as a brand-name drug) are considered *bioequivalent* if their rate and extent of absorption, as quantified by pharmacokinetic parameters, are sufficiently close (Du and Choi 2015). Several approaches have been considered for the assessment of bioequivalence (see e.g., Meyners 2012 for a review), among which the Two One-Sided Tests (TOST) procedure has emerged as the most widely employed approach (Berger and Hsu 1996). This experimental and statistical framework is recognized by the United States Food and Drug Administration (FDA), the European Medicines Agency (EMA), and other regulatory authorities for the approval of generic drugs or new formulations of existing drugs. Importantly, bioequivalence is also used in other critical situations throughout the drug development life-cycle (e.g., pre-clinical and clinical development, manufacturing and quality control, pharmacovigilance, etc.).

In this work, we propose a new approach for multivariate equivalence testing, an area where few methods have been developed. A key motivation for this new approach is the assessment of bioequivalence for locally acting drugs, which are medications designed to exert their therapeutic effects at the site of application without significant systemic absorption. These drugs are not intended to be absorbed into the bloodstream and have local sites of action such as the skin, the eyes, the ears, or the mucosal surfaces of the nose and the lungs, minimizing systemic side effects and drug interactions and thus contributing to safer and more effective therapies. The

assessment of bioequivalence for locally acting drugs is crucial for researchers, regulatory agencies, and generic drug manufacturers (see e.g., [Patil et al. 2021](#), [Mehta et al. 2023](#), [Babiskin et al. 2023](#)). However, establishing bioequivalence for these drugs poses significant challenges, since pharmacokinetic parameters, which are crucial for systemically acting drugs, are only indicative of unintended side effects and are not reliable metrics for assessing bioequivalence in this context (see e.g., [Herkenne et al. 2008](#), [Cordery et al. 2017](#)), leading to more complex, labor-intensive, and time-consuming experimental protocols and thus to smaller sample sizes. Consequently, there are relatively fewer generic products for locally acting drug products, and there is an urgent need for adequate experimental and statistical methods to address this challenge ([Miranda et al. 2018a](#)). Recently, this limitation was recognized by the FDA and the EMA, which have called for innovative methods to evaluate bioequivalence for locally acting drugs, particularly topical formulations (see [EMA 2018](#), [FDA 2022](#), [Volontè et al. 2024](#)). Indeed, the complexity of the underlying clinical protocols leads to large experimental noise which, combined with the multivariate nature of such data, renders classical bioequivalence methods, such as the TOST, to have virtually nil statistical power.

1.1 Main results and contributions

In this paper, we propose a novel finite-sample adjustment for multivariate average equivalence testing problems, which also applies to univariate settings as a special case. To mitigate the conservativeness of the TOST procedure while preserving its simplicity, our proposal matches its test size to the nominal significance level by simultaneously adjusting both the test level and the equivalence margins in use. The proposed approach, which we denote as *corrected TOST* (cTOST), leads to a test procedure with superior operating characteristics compared to the conventional TOST and other existing methods.

In univariate settings, we show that all adjusted TOST procedures are equivalent when the nuisance parameter (i.e., the variance) is assumed to be known. When this parameter is unknown but still employed to characterize the theoretical test size of TOST, we show that the proposed cTOST leads to the optimal adjustment, in the sense that it leads to a uniformly most powerful test procedure. In practice, when the nuisance parameter is replaced by a plugin estimate, we demonstrate that the resulting cTOST maintains such optimal properties in large samples. Nevertheless, in the presence of very small sample sizes, we observe that it may lead to a slightly liberal test procedure. We thus propose a further small-sample refinement that ensures control of the test size while still maintaining desirable properties.

Building on our findings from the univariate case, we extend our focus to the more

complex multivariate setting. We demonstrate that no uniformly most powerful test exists and that locally optimal solutions often yield impractical rejection regions. We thus propose a constrained optimization framework that balances theoretical optimality with practical considerations. By controlling the marginal test sizes across dimensions, our approach yields a computationally efficient adjustment that is both optimal in important cases and practically meaningful. Moreover, the proposed small-sample refinement can be also applied to the multivariate setting.

Finally, we apply the proposed cTOST to multivariate bioequivalence assessments in the context of locally acting drugs, where the underlying labor-intensive and time-consuming experimental protocols severely limit the amount of available data. Unlike existing methods, cTOST can effectively tackle the large experimental noise and achieve a declaration of bioequivalence when other methods fail. We present a real data example of the cutaneous biodistribution between two antifungal topical products for different targeted skin layers (Quartier et al. 2019). This case study illustrates the lack of statistical power in classical bioequivalence testing procedures and showcases the superior operating characteristics achieved by cTOST.

All our new testing procedures are readily available for public usage through the cTOST package in R, which is also available on the GitHub repository <https://github.com/stephaneguerrier/cTOST>.

1.2 Organization

The rest of the article is organized as follows. Section 2 briefly reviews the framework for multivariate equivalence testing as well as the TOST and other existing procedures, considering the univariate setting as a special case. In Section 3, we introduce our cTOST proposal for univariate and multivariate equivalence testing problems, where we also demonstrate its theoretical properties and connections with existing methods, and present a further small-sample refinement. Section 4 includes extensive simulation studies comparing the performance of different methods, and Section 5 contains the assessment of bioequivalence for two antifungal topical products. Finally, some concluding remarks are discussed in Section 6.

2 Average Equivalence Testing Framework

To demonstrate average equivalence, the hypotheses of interest are given by

$$H_0 : \boldsymbol{\theta} \notin (-c_0, c_0)^K \quad \text{vs.} \quad H_1 : \boldsymbol{\theta} \in (-c_0, c_0)^K, \quad (1)$$

where $\boldsymbol{\theta}$ denotes the target equivalence K -dimensional vector and c_0 is a given constant based on expert domain knowledge. For example, in bioequivalence studies, this value could be a standard set by regulatory agencies allowing to quantify how “close” two drugs must be to be declared bioequivalent. Without loss of generality,

we restrict our attention to the conventional choice of equivalence margins that are equal across the K components and symmetric around zero (see e.g., [Berger and Hsu 1996](#), [Pallmann and Jaki 2017](#) and the references therein).

To test the hypotheses in (1), a common assumption (see e.g., [Schuirmann 1987](#), [Jones and Kenward 2003](#), [Wang et al. 1999](#)) is that an estimator of $\boldsymbol{\theta}$, say $\widehat{\boldsymbol{\theta}}$, is available and satisfies the following canonical form:

$$\widehat{\boldsymbol{\theta}} \sim \mathcal{N}_K(\boldsymbol{\theta}, \boldsymbol{\Sigma}_1) \quad \text{and} \quad \nu_2 \widehat{\boldsymbol{\Sigma}}_1 \sim W_K(\boldsymbol{\Sigma}_1, \nu_2), \quad (2)$$

where the two random variables respectively following the normal and the Wishart distribution are independent. Here $\boldsymbol{\Sigma}_1 \equiv \boldsymbol{\Sigma}/\nu_1$ denotes the covariance matrix of $\widehat{\boldsymbol{\theta}}$, which we assume to be positive definite, and $\nu_1 > 0, \nu_2 > 0$ are degrees of freedom related to the sample size, $\nu_1 \asymp \nu_2 \asymp n$, where $u_n \asymp v_n$ indicates that there exist positive constants m_l, m_u and N such that $m_l \leq |u_n/v_n| \leq m_u$ for all $n > N$. For example, when $K = 1$ and the data X_1, \dots, X_n satisfy $E(X_i) = \theta$, then we usually have $\widehat{\theta} = \bar{X} = n^{-1} \sum_{i=1}^n X_i \sim \mathcal{N}(\theta, \sigma_1^2)$, $\sigma^2 \equiv \Sigma = \text{var}(X)$, $\sigma_1^2 = \text{var}(X)/n$, $\nu_1 = n$, $\nu_2 = n - 1$, $\widehat{\sigma}_1^2 = \sum_{i=1}^n (X_i - \bar{X})^2 / \{n(n - 1)\}$, and $\nu_2 \widehat{\sigma}_1^2 / \sigma_1^2 \sim \chi_{\nu_2}^2$ (where the latter denotes a chi-square distribution with ν_2 degrees of freedom). More complex (regression) settings can also be summarized into the above form (see e.g., [Counsell and Cribbie 2015](#) and the references therein) either exactly or in an asymptotic sense.

Several approaches have been considered for univariate average equivalence test-

ing (i.e., when $K = 1$; see e.g., [Meyners 2012](#) for a review), among which TOST procedure has emerged as the most widely adopted approach ([Schuirmann 1987](#), [Berger and Hsu 1996](#)). This procedure requires to compute the following two test statistics: $T_L \equiv (\hat{\theta} + c_0)/\hat{\sigma}_1$ and $T_U \equiv (\hat{\theta} - c_0)/\hat{\sigma}_1$, where T_L tests for $H_{01} : \theta \leq -c_0$ versus $H_{11} : \theta > -c_0$, and T_U tests for $H_{02} : \theta \geq c_0$ versus $H_{12} : \theta < c_0$. At a significance level $\alpha_0 \in (0, 1/2]$, the TOST rejects $H_0 \equiv H_{01} \cup H_{02}$ in favor of $H_1 \equiv H_{11} \cap H_{12}$ if both tests simultaneously reject their marginal null hypotheses, that is, if $T_L \geq t_{\alpha_0, \nu_2}$ and $T_U \leq -t_{\alpha_0, \nu_2}$, where t_{α_0, ν_2} denotes the upper α_0 quantile of a t -distribution with ν_2 degrees of freedom. Both tests are designed to control the false positive rate (type I error rate) at α_0 . Hence, the intersection-union principle guarantees that the resulting TOST procedure is indeed level α_0 ([Berger and Hsu 1996](#)). In practice, the most common way of assessing (and visualizing) bioequivalence is to use the Interval Inclusion Principle (IIP) and accept bioequivalence if the $1 - 2\alpha_0$ confidence interval for θ falls entirely within the equivalence margins $(-c_0, c_0)$; see e.g., [Wellek \(2010\)](#).

The rejection region of the (univariate) TOST procedure is given by

$$C \equiv \left\{ \hat{\theta} \in \mathbb{R}, \hat{\sigma}_1 \in \mathbb{R}_{>0} : t_{\alpha_0, \nu_2} \hat{\sigma}_1 - c_0 < \hat{\theta} < c_0 - t_{\alpha_0, \nu_2} \hat{\sigma}_1 \right\}.$$

Therefore, given α_0 , θ , σ_1 , ν_2 and c_0 , the probability of rejecting H_0 can be expressed

as (see e.g., [Phillips 2009](#))

$$\begin{aligned} \omega(\theta, \sigma_1, \nu_2, t_{\alpha_0, \nu_2}, c_0) &\equiv \Pr(t_{\alpha_0, \nu_2} \widehat{\sigma}_1 - c_0 < \widehat{\theta} < c_0 - t_{\alpha_0, \nu_2} \widehat{\sigma}_1) \\ &= \int I(\widehat{\sigma}_1 t_{\alpha_0, \nu_2} < c_0) \left\{ \Phi \left(\frac{c_0 - t_{\alpha_0, \nu_2} \widehat{\sigma}_1 - \theta}{\sigma_1} \right) - \Phi \left(\frac{t_{\alpha_0, \nu_2} \widehat{\sigma}_1 - c_0 - \theta}{\sigma_1} \right) \right\} f_{\widehat{\sigma}_1}(\widehat{\sigma}_1 | \sigma_1, \nu_2) d\widehat{\sigma}_1, \end{aligned} \quad (3)$$

where $I(\cdot)$ denotes the indicator function with $I(A) = 1$ if A is true and zero otherwise, $\Phi(\cdot)$ denotes the cumulative distribution function of a standard normal distribution, and $f_{\widehat{\sigma}_1}(\cdot)$ is the density of $\widehat{\sigma}_1$. Subsequently, the size of the test is defined as the supremum of $\omega(\theta, \sigma_1, \nu_2, t_{\alpha_0, \nu_2}, c_0)$ over the space of the null hypothesis (see e.g., [Lehmann 1986](#)). It can be shown that for a given σ_1 we have

$$\sup_{\theta \notin (-c_0, c_0)} \omega(\theta, \sigma_1, \nu_2, t_{\alpha_0, \nu_2}, c_0) = \sup_{\theta \in [c_0, \infty)} \omega(\theta, \sigma_1, \nu_2, t_{\alpha_0, \nu_2}, c_0) = \omega(c_0, \sigma_1, \nu_2, t_{\alpha_0, \nu_2}, c_0) < \alpha_0, \quad (4)$$

indicating that TOST is a conservative procedure in the sense that its size is strictly smaller than the target level α_0 (see e.g., [Deng and Zhou 2020](#)). A few strategies have been considered to tackle the conservativeness of the univariate TOST procedure. In the context of bioequivalence, some approaches considered the adjustments of regulatory margins; see for instance [Tothfalusi et al. \(2009\)](#), [Davit et al. \(2012\)](#), [Muñoz et al. \(2016\)](#), [Labes and Schütz \(2016\)](#), [Schütz et al. \(2022\)](#). However, these approaches tend to provide overly liberal test procedures while maintaining a limited power ([Ocaña and Muñoz 2019](#)). Recently, the α -TOST and δ -TOST procedures

were proposed in [Boulaguiem et al. \(2024\)](#) to consider either an adjusted test level, say α^* , or adjusted equivalence margins, say c^* , respectively. However, these adjustments only partially mitigate the conservativeness of TOST and remain suboptimal. Alternatives to TOST could also be considered, but they tend to give overly liberal testing procedures, can be difficult to compute ([Anderson and Hauck 1983](#)), and are typically difficult to interpret as they do not respect the IIP ([Berger and Hsu 1996](#)).

Notably, fewer approaches have been proposed for assessing average equivalence in multivariate settings (i.e., when $K > 1$; see e.g., [Tseng 2002](#), [Chervoneva et al. 2007](#), [Wellek 2010](#) and the references therein). Among these, the multivariate TOST procedure stands out as the most effective method as demonstrated by [Pallmann and Jaki \(2017\)](#) empirically. It relies on test statistics: $T_{L_k} \equiv (\hat{\theta}_k + c_0)/\hat{\sigma}_{1,k}$ and $T_{U_k} \equiv (\hat{\theta}_k - c_0)/\hat{\sigma}_{1,k}$, for $k = 1, \dots, K$, where $\hat{\sigma}_{1,k}^2$ is the k th diagonal element of $\hat{\Sigma}_1$, and rejects H_0 if each of the K marginal TOSTs rejects its marginal null hypothesis. Similarly to the univariate case, the IIP ensures that equivalence can be declared when each marginal confidence interval for θ_k , where $k = 1, \dots, K$, is entirely contained within the equivalence margins $(-c_0, c_0)$. At a significance level α_0 , the multivariate TOST has the rejection region of the form

$$C_K \equiv \left\{ \hat{\boldsymbol{\theta}} \in \mathbb{R}^K, (\hat{\sigma}_{1,1}, \dots, \hat{\sigma}_{1,K})^T \in \mathbb{R}_{>0}^K : \bigcap_{k=1}^K \left(t_{\alpha_0, \nu_2} \hat{\sigma}_{1,k} - c_0 < \hat{\theta}_k < c_0 - t_{\alpha_0, \nu_2} \hat{\sigma}_{1,k} \right) \right\},$$

which is derived from an extension of the univariate TOST to the multivariate

framework (Berger 1982). Then, the probability of rejecting H_0 for the multivariate TOST (see e.g., Phillips 2009) can be expressed as $\omega_K(\boldsymbol{\theta}, \boldsymbol{\Sigma}_1, \nu_2, t_{\alpha_0, \nu_2}, c_0) \equiv \Pr(\widehat{\boldsymbol{\theta}} \in C_K | \boldsymbol{\theta}, \boldsymbol{\Sigma}_1, \nu_2, \alpha_0, c_0)$. While the multivariate TOST remains easier to interpret and exhibits greater power compared to other testing procedures (Pallmann and Jaki 2017), its conservativeness persists and in fact becomes more pronounced when applied to multivariate equivalence problems. This increased conservativeness suggests improvement opportunities and motivates the development of further refinements.

3 Towards an Optimally Corrected TOST: cTOST

In this section, we detail the derivation and theoretical properties of the proposed cTOST, its advantages over existing methods and its practical implications. While the aim is optimality, the multivariate context presents unique challenges. Therefore, we first focus on the univariate setting, demonstrating that the proposed cTOST leads to an optimal adjustment. We then extend our approach to the more complex multivariate framework where, although we establish that an optimal adjustment does not exist, cTOST maintains a degree of optimality in important cases. Moreover, to control its properties in small samples, we introduce an additional refinement step ensuring that cTOST does not lead to a liberal test procedure.

3.1 Univariate cTOST

We aim at constructing an optimal adjustment for the TOST, in the sense that it achieves a size equal to the nominal significance level α_0 while simultaneously maximizing the power of the test – i.e., the probability of rejecting H_0 when $\theta \in (-c_0, c_0)$. To achieve this, we consider a more flexible rejection region by treating c_0 and the α_0 in t_{α_0, ν_2} as parameters c, α to get

$$C(\alpha, c) \equiv \left\{ \widehat{\theta} \in \mathbb{R}, \widehat{\sigma}_1 \in \mathbb{R}_{>0} : t_{\alpha, \nu_2} \widehat{\sigma}_1 - c < \widehat{\theta} < c - t_{\alpha, \nu_2} \widehat{\sigma}_1 \right\}, \quad (5)$$

and then match the size function in (4) to the nominal level α_0 by requiring that $\omega(c_0, \sigma_1, \nu_2, t_{\alpha, \nu_2}, c) = \alpha_0$. This results in a set $\mathcal{A}(\alpha_0)$ of possible adjustments, formally defined as

$$\mathcal{A}(\alpha_0) \equiv \{(\alpha, c) : \alpha \in (0, 0.5], c \in \mathbb{R}_{>0}, \omega(c_0, \sigma_1, \nu_2, t_{\alpha, \nu_2}, c) = \alpha_0\}. \quad (6)$$

We note that the size function $\omega(c_0, \sigma_1, \nu_2, t_{\alpha, \nu_2}, c)$ has the property that, at any fixed $t_{\alpha, \nu_2} \in [0, \infty)$, it is a strictly increasing and differentiable function of c , and has value 0 at $c = 0$ and value 1 as $c \rightarrow \infty$. Hence, for any $t_{\alpha, \nu_2} \in [0, \infty)$, there exists a unique value of c , denoted as $c(t_{\alpha, \nu_2}, \nu_2)$, so that $\omega\{c_0, \sigma_1, \nu_2, t_{\alpha, \nu_2}, c(t_{\alpha, \nu_2}, \nu_2)\} = \alpha_0$. Thus, $\mathcal{A}(\alpha_0) = \{(\alpha, c(t_{\alpha, \nu_2}, \nu_2))\}$, where $\alpha \in (0, 0.5]$, and we aim at finding the optimal α so that the power $\omega\{\theta, \sigma_1, \nu_2, t_{\alpha, \nu_2}, c(t_{\alpha, \nu_2}, \nu_2)\}$ is maximized for $\theta \in (-c_0, c_0)$. Finding

such optimal α is equivalent to finding the corresponding optimal t_{α, ν_2} value, so we simplify the above problem as finding t so that $\omega\{\theta, \sigma_1, \nu_2, t, c(t, \nu_2)\}$ is maximized for $\theta \in (-c_0, c_0)$. The solution is surprisingly simple, in that we find the optimal t is simply zero for all $\theta \in (-c_0, c_0)$. Specifically, for notational simplicity, we define

$$c(0) \equiv c(0, \nu_2) = \underset{c \in \mathbb{R}_{>0}}{\text{argzero}} \{\omega(c_0, \sigma_1, \nu_2, 0, c) - \alpha_0\}. \quad (7)$$

We find that setting c at $c(0)$ leads to the optimal power. While the result is formally given in Theorem 1, we now provide some intuition behind. In the α -TOST procedure, which also belongs to the set of adjustments $\mathcal{A}(\alpha_0)$ in (6), it was shown that an increase in α leads to more powerful test procedures compared to an increase in c . The maximum value at $\alpha = 1/2$ is then a natural candidate. Moreover, the power function at $\alpha = 1/2$, which is $\omega(\theta, \sigma_1, \nu_2, 0, c)$, coincides with the power function for the known σ_1 case (see Appendix A), which intuitively is the upper bound of the power of the unknown σ_1 case. On the other hand, when σ_1^2 is known, all adjustments that lead to size- α_0 procedures have equal power under H_1 (see Appendix A for details), and they are equivalent to the uniformly most powerful test presented in Romano (2005). This observation indicates that the adjustment in (7) leads to the uniformly most powerful test procedure, as demonstrated in Theorem 1.

Theorem 1: *For any given ν_2 and σ_1 , $c(0)$ defined in (7) satisfies $\omega\{\theta, \sigma_1, \nu_2, t, c(t, \nu_2)\} \leq$*

$\omega\{\theta, \sigma_1, \nu_2, 0, c(0)\}$, for any $t > 0$, where $\{t, c(t, \nu_2)\} \in \mathcal{A}(\alpha_0)$ in (6), and any $\theta \in (-c_0, c_0)$.

The proof of Theorem 1 is presented in Appendix B. Theorem 1 indicates that among all level- α_0 tests, cTOST is the uniformly most powerful test. In addition to its superiority in terms of power, cTOST offers substantial computational gain compared to the existing adjusted TOST procedures, which often require the computation of an additional integral over the space of $\hat{\sigma}_1$ as given in (3). Although Theorem 1 considers the case that σ_1 is unknown, the resulting solution, i.e., the optimal choice $c(0)$, depends on the true σ_1 value, which in practice we replace by

$$\hat{c}(0) \equiv \underset{c \in \mathbb{R}_{>0}}{\text{argzero}} \{ \omega(c_0, \hat{\sigma}_1, \nu_2, 0, c) - \alpha_0 \}. \quad (8)$$

For simplicity, we still refer to the resulting procedure as cTOST even though it now relies on $\hat{\sigma}_1$ instead of σ_1 . Similarly, we let $\hat{c}(t, \nu_2)$ satisfy $\omega\{c_0, \hat{\sigma}_1, \nu_2, t_{\alpha, \nu_2}, \hat{c}(t, \nu_2)\} = \alpha_0$. To show that the substitution of σ_1 by $\hat{\sigma}_1$ does not harm the performance of cTOST and that it remains the optimal adjustment in large samples, we first establish some preliminary results in Proposition 1.

Proposition 1: *For any $t > 0$, we have:*

1. $\hat{c}(0) - c(0) = O_p(\sigma_1/\sqrt{\nu_2})$,
2. $\hat{c}(t, \nu_2) - c(t, \nu_2) = O_p(\sigma_1/\sqrt{\nu_2})$,

$$3. |c(0) - \{c(t, \nu_2) - t\hat{\sigma}_1\}| \asymp \sigma_1.$$

The proof of Proposition 1 is given in Appendix C. Proposition 1 indicates that for large n , the difference between $\hat{c}(0)$ and $c(0)$ (result 1) caused by estimating σ_1 , as well as the difference between $\hat{c}(t, \nu_2)$ and $c(t, \nu_2)$ for a general t (result 2), are ignorable compared to the difference caused by choosing a nonzero t versus a zero t value (result 3, see (5)), which is what cTOST does. Thus, the $\hat{c}(0)$ adjustment still has the optimal power property while retaining the size α_0 in large samples. This result is formally shown in the following theorem.

Theorem 2: $\hat{c}(0)$ defined in (8) satisfies:

$$1. \text{ For any } t \geq 0, \omega\{c_0, \sigma_1, \nu_2, t, \hat{c}(t, \nu_2)\} = \alpha_0 + O_p(\nu_2^{-1/2}).$$

$$2. \text{ For any } t > 0, \text{ and any } \theta \in (-c_0, c_0), \text{ when } \nu_2 \text{ is sufficiently large, } \omega\{\theta, \sigma_1, \nu_2, t, \hat{c}(t, \nu_2)\} \leq \omega\{\theta, \sigma_1, \nu_2, 0, \hat{c}(0)\}.$$

The proof of Theorem 2 is given in Appendix D. The first part of Theorem 2 implies that the asymptotic size of the corrected procedure is α_0 . The second part of this result shows that with only an estimated σ_1 available, for large n , setting α to 1/2 still leads to the optimal adjustment. In practice, $\hat{c}(0)$ can be efficiently computed using, for instance, the Newton-Raphson method described in Appendix E. Then, if $|\hat{\theta}| < \hat{c}(0)$, we accept H_1 at the significance level α_0 .

3.2 Multivariate cTOST

Similarly to the univariate case, it is easy to see that the multivariate TOST is conservative, meaning that its size, which can be derived from (10)-(11) below, is strictly smaller than the nominal level α_0 . Following the univariate cTOST idea, for each $k = 1, \dots, K$, we relax the marginal test rejection regions to $\{\widehat{\theta}_k, \widehat{\sigma}_{1,k} : t\widehat{\sigma}_{1,k} - c < \widehat{\theta} < c - t\widehat{\sigma}_{1,k}\}$. This leads to the multivariate test rejection region of the form

$$C_K(\mathbf{t}, \mathbf{c}) \equiv \left\{ \widehat{\boldsymbol{\theta}} \in \mathbb{R}^K, (\widehat{\sigma}_{1,1}, \dots, \widehat{\sigma}_{1,K})^T \in \mathbb{R}_{>0}^K : \bigcap_{k=1}^K \left(t_k \widehat{\sigma}_{1,k} - c_k < \widehat{\theta}_k < c_k - t_k \widehat{\sigma}_{1,k} \right) \right\},$$

where $\mathbf{t} \equiv (t_1, \dots, t_K)^T$ and $\mathbf{c} \equiv (c_1, \dots, c_K)^T$. We denote the probability of rejecting H_0 as

$$\begin{aligned} \omega_K(\boldsymbol{\theta}, \boldsymbol{\Sigma}_1, \nu_2, \mathbf{t}, \mathbf{c}) &\equiv \Pr\{(\widehat{\boldsymbol{\theta}}, \widehat{\sigma}_{1,1}, \dots, \widehat{\sigma}_{1,K})^T \in C_K(\mathbf{t}, \mathbf{c})\} \\ &= \Pr \left\{ \bigcap_{k=1}^K \left(\frac{t_k \widehat{\sigma}_{1,k} - c_k}{\sigma_{1,k}} - \frac{\theta_k}{\sigma_{1,k}} < \frac{\widehat{\theta}_k - \theta_k}{\sigma_{1,k}} < \frac{c_k - t_k \widehat{\sigma}_{1,k}}{\sigma_{1,k}} - \frac{\theta_k}{\sigma_{1,k}} \right) \right\}. \end{aligned} \quad (9)$$

Note that $\widehat{\sigma}_{1,k}$ involves ν_2 , hence ω_K is a function of ν_2 as well. To control the size of the test at α_0 , we restrict ourselves to the set $\mathcal{A}_K^*(\alpha_0)$, where

$$\mathcal{A}_K^*(\alpha_0) \equiv \{(\mathbf{t}, \mathbf{c}) : \mathbf{t} \in \mathbb{R}_{\geq 0}^K, \mathbf{c} \in \mathbb{R}_{>0}^K, \omega_K\{\boldsymbol{\lambda}(\mathbf{t}, \mathbf{c}), \boldsymbol{\Sigma}_1, \nu_2, \mathbf{t}, \mathbf{c}\} = \alpha_0\}, \quad (10)$$

and $\boldsymbol{\lambda}(\mathbf{t}, \mathbf{c}) \equiv (\lambda_1, \dots, \lambda_K)^T \in \boldsymbol{\Lambda}(\boldsymbol{\Sigma}_1, \nu_2, \mathbf{t}, \mathbf{c}) \equiv \underset{\boldsymbol{\theta} \notin (-c_0, c_0)^K}{\text{argsup}} \omega_K(\boldsymbol{\theta}, \boldsymbol{\Sigma}_1, \nu_2, \mathbf{t}, \mathbf{c}). \quad (11)$

Here $\boldsymbol{\lambda}(\mathbf{t}, \mathbf{c})$ also depends on $\boldsymbol{\Sigma}_1$ and ν_2 , while we omit them for notational simplicity. Note that the complement set of $(-c_0, c_0)^K$ is the parameter space under the null hypothesis, hence $\boldsymbol{\lambda}(\mathbf{t}, \mathbf{c})$ defined in (11) leads to the worst-case scenario of the rejection probability under H_0 . In the univariate case ($K = 1$), it is obvious that $\lambda(t, c) = \pm c_0$, and we can simply consider $\lambda(t, c) = c_0$ for subsequent power analysis without loss of generality. However, in the multivariate case ($K > 1$), other than $\boldsymbol{\lambda}(\mathbf{t}, \mathbf{c})$ being on the boundary of $(-c_0, c_0)^K$, a closed form of $\boldsymbol{\lambda}(\mathbf{t}, \mathbf{c})$ is not attainable in general due to its complex relation to $\boldsymbol{\Sigma}_1$. See Appendix F for an illustration of how $\boldsymbol{\lambda}(\mathbf{t}, \mathbf{c})$ is affected by the correlation in $\boldsymbol{\Sigma}_1$.

In contrast to the univariate case, even for a fixed \mathbf{t} in (10), there exists multiple $\mathbf{c}(\mathbf{t})$'s, where $\mathbf{c}(\mathbf{t}) \equiv [c_1(\mathbf{t}), \dots, c_K(\mathbf{t})]^T$, that guarantee the size α_0 simply because we have only a single requirement $\omega_K[\boldsymbol{\lambda}\{\mathbf{t}, \mathbf{c}(\mathbf{t})\}, \boldsymbol{\Sigma}_1, \nu_2, \mathbf{t}, \mathbf{c}(\mathbf{t})] = \alpha_0$ while we have $K > 1$ degrees of freedom in $\mathbf{c}(\mathbf{t})$. Indeed, if we start from a rejection region based on any $\{\mathbf{t}, \mathbf{c}(\mathbf{t})\} \in \mathcal{A}_K^*(\alpha_0)$, then it is always possible to increase the rejection region across some dimensions while reducing it along some other dimensions to preserve the size of α_0 . In particular, highly unbalanced rejection region can occur, where some entries of $\mathbf{c}(\mathbf{t})$ may exceed c_0 while others can be arbitrarily close to 0 (see Appendix F for an example), which may not be desirable in practice. Thus, in addition to achieving an overall size of α_0 , we further impose an equal marginal size requirement, i.e., $\omega\{c_0, \sigma_{1,k}, \nu_2, t_k, c_k(\mathbf{t})\}$ are identical across all $k = 1, \dots, K$. The

marginal size can be viewed as the size of the univariate test concerning only the k th component of $\boldsymbol{\theta}$. This leads to the reduced set

$$\begin{aligned} \mathcal{A}_K(\alpha_0) \equiv \{(\mathbf{t}, \mathbf{c}) : \mathbf{t} \in \mathbb{R}_{\geq 0}^K, \mathbf{c} \in \mathbb{R}_{> 0}^K, \omega_K\{\boldsymbol{\lambda}(\mathbf{t}, \mathbf{c}), \boldsymbol{\Sigma}_1, \nu_2, \mathbf{t}, \mathbf{c}\} = \alpha_0, \\ \omega(c_0, \sigma_{1,1}, \nu_2, t_1, c_1) = \cdots = \omega(c_0, \sigma_{1,K}, \nu_2, t_K, c_K)\}. \end{aligned} \quad (12)$$

For a fixed \mathbf{t} , there is a unique solution $\mathbf{c}(\mathbf{t})$ so that $\{\mathbf{t}, \mathbf{c}(\mathbf{t})\} \in \mathcal{A}_K(\alpha_0)$. Building upon the univariate setting presented in Section 3.1, one can expect that among all potential $\{\mathbf{t}, \mathbf{c}(\mathbf{t})\} \in \mathcal{A}_K(\alpha_0)$, setting $\mathbf{t} = \mathbf{0}$ would lead to some desirable properties. This prompts us to consider $\mathbf{c}^* \equiv \mathbf{c}(\mathbf{0})$ such that

$$\omega_K\{\boldsymbol{\lambda}(\mathbf{0}, \mathbf{c}^*), \boldsymbol{\Sigma}_1, \nu_2, \mathbf{0}, \mathbf{c}^*\} = \alpha_0, \quad (13)$$

$$\text{where } \boldsymbol{\lambda}(\mathbf{0}, \mathbf{c}^*) \in \Lambda(\boldsymbol{\Sigma}_1, \nu_2, \mathbf{0}, \mathbf{c}^*) \equiv \operatorname{argsup}_{\boldsymbol{\theta} \notin (-c_0, c_0)^K} \omega_K(\boldsymbol{\theta}, \boldsymbol{\Sigma}_1, \nu_2, \mathbf{0}, \mathbf{c}^*), \quad (14)$$

$$\text{and } \omega(c_0, \sigma_{1,1}, \nu_2, 0, c_1^*) = \cdots = \omega(c_0, \sigma_{1,K}, \nu_2, 0, c_K^*) = \gamma. \quad (15)$$

Interestingly, we will always have $\gamma \geq \alpha_0$, as the global size in (13) cannot exceed the marginal sizes in (15), i.e.,

$$\begin{aligned} \alpha_0 = \omega_K\{\boldsymbol{\lambda}(\mathbf{0}, \mathbf{c}^*), \boldsymbol{\Sigma}_1, \nu_2, \mathbf{0}, \mathbf{c}^*\} &\leq \min_{k=1, \dots, K} \omega\{\lambda_k(\mathbf{0}, \mathbf{c}^*), \sigma_{1,k}, \nu_2, 0, c_k^*\} \\ &\leq \omega\{\lambda_h(\mathbf{0}, \mathbf{c}^*), \sigma_{1,h}, \nu_2, 0, c_h^*\} = \gamma. \end{aligned}$$

The first inequality is a Fréchet inequality, the second inequality holds since $\boldsymbol{\lambda}(\mathbf{0}, \mathbf{c}^*)$

has at least one entry, say h , at $\pm c_0$ to satisfy (14), and the first and last equalities are respectively defined in (13) and (15). We denote the proposed adjusted TOST under the $(\mathbf{0}, \mathbf{c}^*) \in \mathcal{A}_K(\alpha_0)$ choice as multivariate cTOST. Similarly to the univariate cTOST, for the multivariate cTOST, the probability of rejecting H_0 , $\omega_K(\boldsymbol{\theta}, \boldsymbol{\Sigma}_1, \nu_2, \mathbf{0}, \mathbf{c}^*)$, does not change if $\boldsymbol{\Sigma}_1$ is known, given that we restrict to the reduced set (12) as well. Furthermore, when $\boldsymbol{\Sigma}_1$ is known, all size- α_0 adjustments with equal marginal sizes possess equal power under H_1 (see Appendix G).

Although the family of adjustments $\{\mathbf{t}, \mathbf{c}(\mathbf{t})\} \in \mathcal{A}_K(\alpha_0)$ guarantees the uniqueness of the test at any fixed \mathbf{t} , no choice of \mathbf{t} can lead to a uniformly most powerful test in this family when $\boldsymbol{\Sigma}_1$ is unknown, as demonstrated in Appendix H. To illustrate the theoretical properties of multivariate cTOST, we restrict our analysis to the scenario of $\hat{\boldsymbol{\theta}}$ with independent homoskedastic components, i.e., $\sigma_{1,1} = \dots = \sigma_{1,K}$. Here, we show in Proposition 2 that among all choices of $\{\mathbf{t}, \mathbf{c}(\mathbf{t})\} \in \mathcal{A}_K(\alpha_0)$, the multivariate cTOST has the largest power when evaluated at the alternative $\boldsymbol{\theta} = \mathbf{0}$, which is of the greatest interest when assessing multivariate bioequivalence.

Proposition 2: *At any given ν_2 , σ_1 , consider $\boldsymbol{\Sigma}_1 = \sigma_1^2 \mathbf{I}_K$. Then for all $\{\mathbf{t}, \mathbf{c}(\mathbf{t})\} \in \mathcal{A}_K(\alpha_0)$ in (12), \mathbf{c}^* defined in (13)-(15) satisfies $\omega_K\{\mathbf{0}, \boldsymbol{\Sigma}_1, \nu_2, \mathbf{t}, \mathbf{c}(\mathbf{t})\} \leq \omega_K\{\mathbf{0}, \boldsymbol{\Sigma}_1, \nu_2, \mathbf{0}, \mathbf{c}^*\}$. Hence, at the origin, the multivariate cTOST is the most powerful test among all the tests defined by $(\mathbf{t}, \mathbf{c}) \in \mathcal{A}_K(\alpha_0)$.*

The proof of Proposition 2 is presented in Appendix H. Proposition 2 ensures

that under independence and homoskedasticity, among all (globally) size- α_0 tests with equal marginal sizes, the multivariate cTOST is the most powerful test at the origin. We conjecture that this optimality property also holds under heteroskedasticity and general correlation structures. Numerical results for bivariate settings support this conjecture (see Appendix H). However, despite its optimality at $\boldsymbol{\theta} = \mathbf{0}$, the multivariate cTOST may become less powerful in some regions of the alternative space, such as the one close to $\boldsymbol{\theta} = c_0 \mathbf{1}_K$ (where $\mathbf{1}_K$ is a length K vector of ones). This result is demonstrated in Appendix H under the same assumptions of Proposition 2. Furthermore, in Appendix I we illustrate the superior operating characteristics of multivariate cTOST versus multivariate α -TOST (Boulaguiem et al. 2025), which belongs to the set $\mathcal{A}_K^*(\alpha_0)$ in (10).

The construction of a feasible finite-sample adjustment $\widehat{\mathbf{c}}^*$ for multivariate cTOST, where population quantities in (13)-(15) are replaced by their empirical counterparts, follows similar procedures to that described in Section 3.1 for the univariate cTOST. Operationally, $\widehat{\mathbf{c}}^*$ can be efficiently computed by leveraging the algorithm for the univariate cTOST described in Appendix E. A formal description of our algorithm is provided in Appendix J. Similarly to the univariate framework, if $|\widehat{\theta}_k| < \widehat{c}_k^*$, for all $k = 1, \dots, K$, H_0 is rejected at the significance level α_0 .

3.3 Further Small-Sample Refinements

For reasonable sample sizes, cTOST in (8) is very accurate at controlling the size of the test, as illustrated in the numerical results of Section 4. Specifically, for most practical applications, where ν_2 is not too small, it effectively maintains the size at α_0 . When sample size is extremely small, cTOST may not adequately control the test size. Given the critical importance of controlling the test size in bioequivalence studies, as it relates to the “consumer” or “regulator” risk (Patterson and Jones 2017), we further refine cTOST so that it maintains the test size even under very limited amount of data.

Specifically, we replace α_0 with a “calibrated” level $\alpha_c \leq \alpha_0$ to further adjust $\widehat{c}(0)$ in (8). The empirical size associated to $\widehat{c}(0, \widehat{\sigma}_1, \alpha_0) \equiv \widehat{c}(0)$ defined in (8) can be expressed as $\omega\{c_0, \sigma_1, \nu_2, 0, \widehat{c}(0, \widehat{\sigma}_1, \alpha_0)\} = \Pr\{|\widehat{\theta}| \leq \widehat{c}(0, \widehat{\sigma}_1, \alpha_0) | \theta = c_0, \sigma_1 = \sigma_1\}$, which incorporates the uncertainty associated with the estimation of σ_1 . This is in contrast to the theoretical size based on a plug-in of $\widehat{\sigma}_1$, that is, $\omega\{c_0, \widehat{\sigma}_1, \nu_2, 0, \widehat{c}(0, \widehat{\sigma}_1, \alpha_0)\} = \Pr\{|\widehat{\theta}| < \widehat{c}(0, \widehat{\sigma}_1, \alpha_0) | \theta = c_0, \sigma_1 = \widehat{\sigma}_1\}$, used to solve the matching in (8). Therefore, a calibrated level α_c can be defined as

$$\alpha_c \equiv \underset{\gamma \in (0, \alpha_0]}{\operatorname{argzero}} E[\omega\{c_0, \widehat{\sigma}_1, \nu_2, 0, \widehat{c}(0, \widehat{\sigma}_1^*, \gamma)\}] - \alpha_0, \quad (16)$$

where $\nu_2 \widehat{\sigma}_1^{*2} / \widehat{\sigma}_1^2 \sim \chi_{\nu_2}^2$ conditionally on $\widehat{\sigma}_1$. A simple iterative approach can be

used to compute α_c , where at each iteration j , with $j \in \mathbb{N}$, we update $\alpha_c^{(j+1)} = \alpha_0 + \alpha_c^{(j)} - E[\omega\{c_0, \hat{\sigma}_1, \nu_2, 0, \hat{c}(0, \hat{\sigma}_1^*, \alpha_c^{(j)})\}]$, initializing the procedure at $\alpha_c^{(0)} = \alpha_0$. In practice, a single iteration is often sufficient to ensure a reliable test size. We then let $\tilde{c}(0)$ denote a refined version of $\hat{c}(0)$ in (8) defined as:

$$\tilde{c}(0) \equiv \hat{c}(0, \hat{\sigma}_1, \alpha_c) = \underset{c \in \mathbb{R}_{>0}}{\text{argzero}} \{ \omega(c_0, \hat{\sigma}_1, \nu_2, 0, c) - \alpha_c \}. \quad (17)$$

Several approaches can be used to approximate the expectation in (16), such as the bootstrap. For given α_0 and c_0 , a precomputed table containing approximations of the expectation in (16), based on a grid of σ_1 and ν_2 values, can be stored in software allowing for efficient computation of $\tilde{\alpha}_c$ (i.e., the empirical counterpart of α_c) without additional computational overhead. For the customary equivalence margins and significance level that are used by regulatory agencies in bioequivalence studies (i.e., $c_0 = \log(1.25) \approx 0.223$ and $\alpha_0 = 0.05$), we provide the resulting table as a part of our software implementation in the `cTOST` R package. Additional details on the small-sample refinement, along with simulation results demonstrating its effectiveness for very small sample sizes (e.g., $\nu_2 = 5$), are presented in Appendix K. When necessary, a similar approach can be applied to multivariate cTOST adjustments \hat{c}^* described in Section 3.2.

4 Simulation Studies

We present the results of extensive univariate and multivariate simulation studies to compare the performance of various methods.

4.1 Univariate Setting

For univariate simulations, we consider the canonical form defined in (2) for $K = 1$. We vary σ_1 over 1000 equally-spaced values in the interval $[0.01, 0.2]$ with degrees of freedom $\nu_2 \in \{20, 40, 80\}$, at the nominal significance level $\alpha_0 = 0.05$ and equivalence bound $c_0 = \log(1.25)$. Four methods are compared: the standard TOST, the α -TOST, the cTOST based on $\widehat{c}(0)$ in (8), and its refined counterpart (cTOST*) based on $\widetilde{c}(0)$ in (17). The study is based on 10^5 Monte Carlo replications.

The empirical size of the different methods is shown in the first row of Figure 1, while their power is evaluated by setting $\theta = 0$, and is in the second row, where we report the power difference between α -TOST, cTOST, and cTOST* relative to the standard TOST. These results demonstrate that both the cTOST* and cTOST can substantially improve the power of the testing procedure compared to the TOST, and to a lesser extent, the α -TOST. While cTOST remains most powerful across all settings, it exhibits a slightly inflated size for small ν_2 's. On the other hand, the empirical size of cTOST* remains consistently close to α_0 , staying within the simulation error bounds of this numerical experiment (represented as gray regions

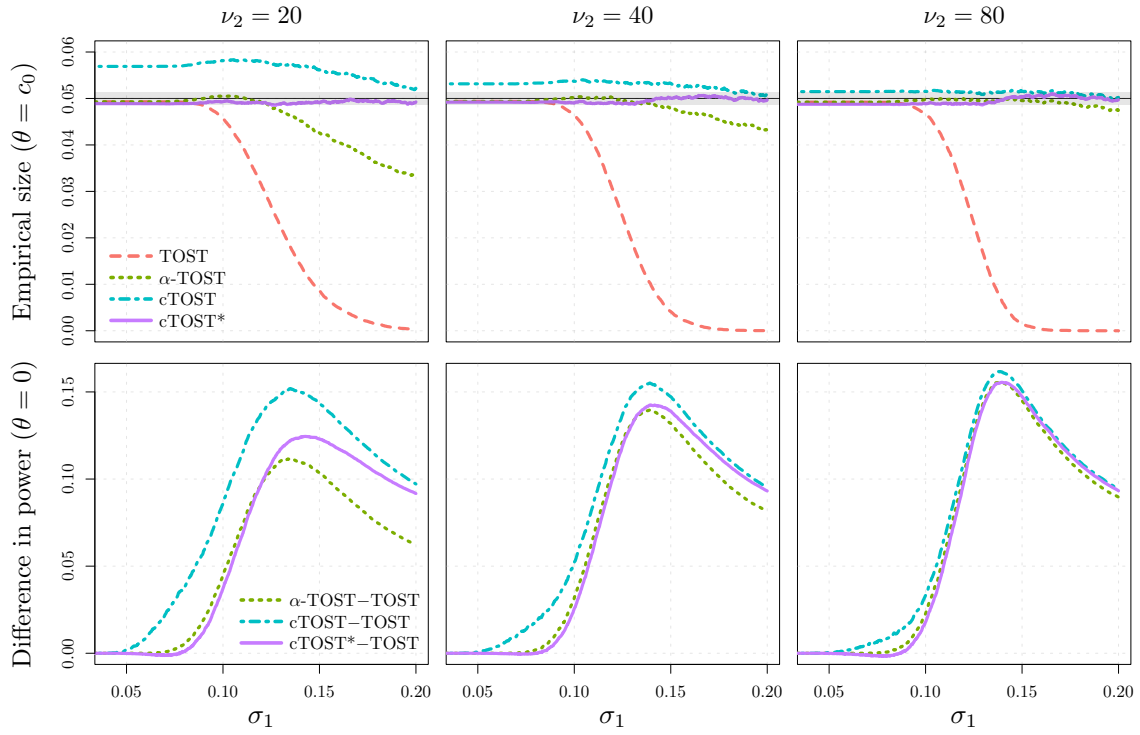


Figure 1: Simulation results comparing the performance of TOST, α -TOST, cTOST and cTOST*. Top row: Empirical size. Bottom row: Difference in power at $\theta = 0$ with respect to TOST.

around the α_0 value, denoted by a black solid line), while still having generally larger power than α -TOST and TOST.

Additional simulation results are presented in Appendix K, where we more closely study the power and size of various test procedures, examine a wider range of θ values, and consider scenarios with fewer degrees of freedom ν_2 . Across all settings, the performance remains consistent with the results presented in Figure 1.

4.2 Multivariate Setting

For multivariate simulations, we consider the canonical form in (2) for $K > 1$. To facilitate a fair comparison across test procedures, we consider $\widehat{\boldsymbol{\theta}} \sim \mathcal{N}_K\{\kappa\boldsymbol{\lambda}, \boldsymbol{\Sigma}_1\}$, where the vector $\boldsymbol{\lambda}$ defined in (11) denotes the coordinates in the parameter space under the null hypothesis that determine the method-specific test size. We then vary the parameter κ across 30 equally-spaced values in the interval $[0, 1.2]$. Therefore, while the test size is evaluated at $\kappa = 1$, the probabilities of declaring equivalence under the alternative and null hypotheses are respectively evaluated at $\kappa \in [0, 1)$ and $\kappa \in (1, 1.2]$. For the covariance matrix $\boldsymbol{\Sigma}_1$, we consider $\Sigma_{1,jk} = \rho\sigma_{1,j}\sigma_{1,k}$ for $j \neq k$ and $\Sigma_{1,jk} = \sigma_{1,j}^2$ otherwise, where $|\rho| < 1$ denotes the pairwise correlation.

We consider two dimensions $K \in \{2, 4\}$, three correlation levels $\rho \in \{0, 0.5, 0.9\}$, and six configurations of the covariance matrix $\boldsymbol{\Sigma}_1 \in \{\boldsymbol{\Sigma}_1^{(1)}, \dots, \boldsymbol{\Sigma}_1^{(6)}\}$. In the bivariate setting, the six configurations are $(\sigma_1, \sigma_2) \in \{(0.08, 0.08), (0.12, 0.12), (0.16, 0.16), (0.08, 0.12), (0.08, 0.16), (0.12, 0.16)\}$. In the 4-variate setting, we set $\sigma_1 = \sigma_2$ and $\sigma_3 = \sigma_4$, where each pair takes the same six sets of values. The study is based on 5×10^4 Monte Carlo replications.

Figure 2 compares the performance of the multivariate TOST and the multivariate cTOST – no further refinement was necessary for cTOST due to its good performance in these settings. Similarly to the univariate case presented in Section 4.1, the multivariate cTOST is more powerful than TOST across all simulation settings

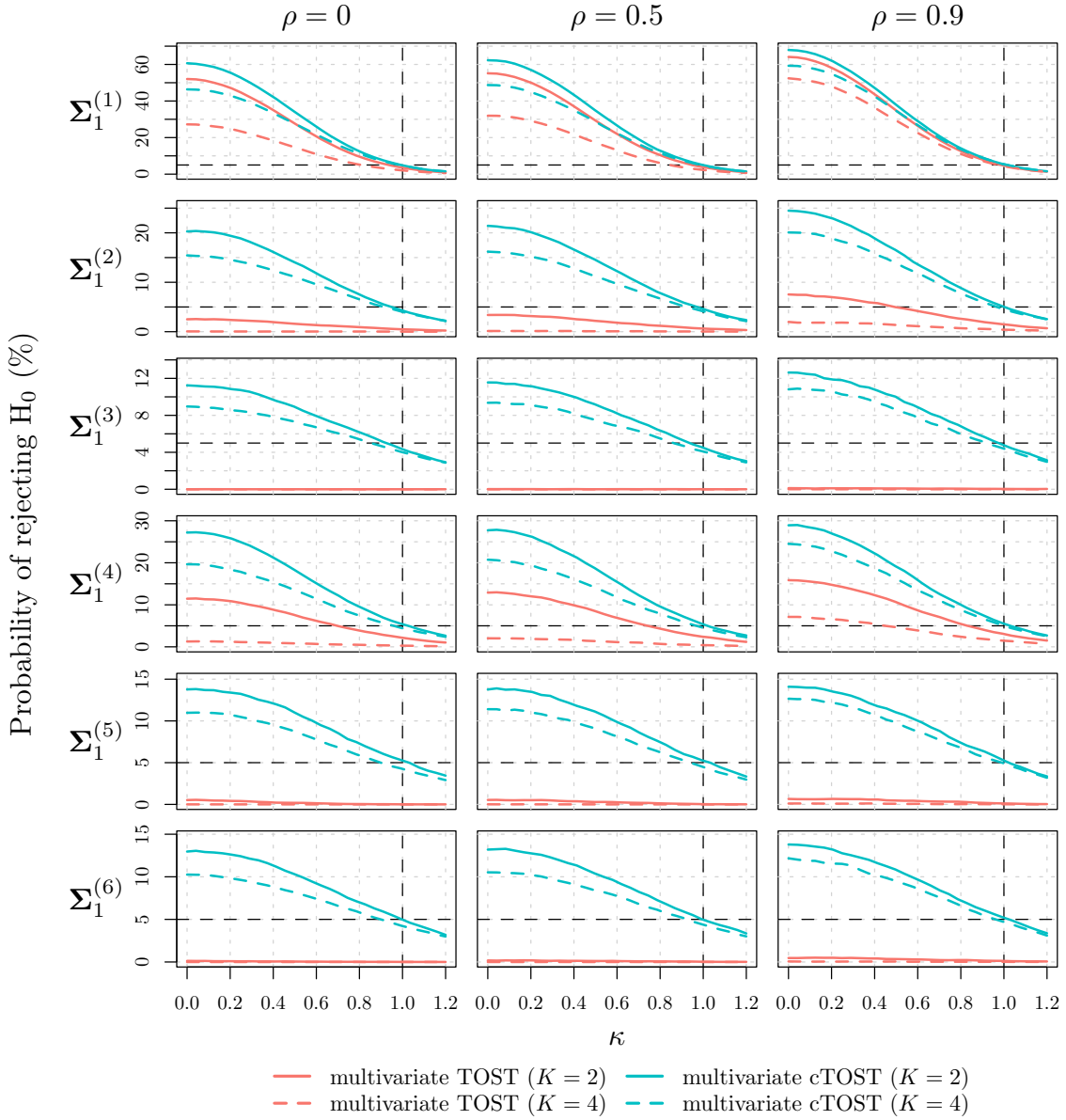


Figure 2: Probability of rejecting the null hypothesis as a function of κ , for the multivariate TOST and the multivariate cTOST, across different levels of correlation ρ (columns) and covariance matrices (rows), for the bivariate (solid lines) and 4-variate (dashed lines) settings.

and, importantly, its empirical size remains very close to the nominal level α_0 . As expected, it provides greater power gains in the presence of lower levels of correlation, higher dimensionality, and larger variances. The multivariate α -TOST performs

better than the multivariate TOST, but it remains less powerful than cTOST across all settings (see Appendix L). Furthermore, the multivariate cTOST offers improved computational efficiency and stability compared to the α -TOST. The latter may also lead to fairly uneven rejection regions (i.e., leading to very different marginal sizes), failing to reflect the practical situations of interest to scientists, as illustrated in the case study in Section 5.

5 Case Study: Cutaneous Bioequivalence

[Quartier et al. \(2019\)](#) conducted a study on the cutaneous bioequivalence between two topical cream products: a brand-name cream (*Pevaryl*) and an approved generic formulation (*Mylan*) containing econazole nitrate (ECZ), an antifungal medication commonly utilized in the treatment of skin infections. The evaluation of putative bioequivalence relies on analyzing the cutaneous biodistribution profile of ECZ following the application of *Pevaryl* versus *Mylan*. This entails quantifying ECZ concentrations at different skin depths, ranging from the surface to a depth of approximately 800 μm . The similarity in biodistribution profiles – indicative of comparable drug concentration at each skin depth – is used to evaluate their bioequivalence. The dataset consists of $n = 12$ independent pairs of comparable porcine skin samples on which ECZ deposition measurements were collected after applying the two topical products. The sample size is heavily limited by the complexity of the experimental

| Multivariate method | <i>Stratum corneum</i> (0–20 μm) | <i>Viable epidermis</i> (20–160 μm) | <i>Upper dermis</i> (160–400 μm) | <i>Lower dermis</i> (400–800 μm) | Bioequivalence declaration |
|---------------------|---|--|---|---|----------------------------|
| TOST | [-0.496, 0.691] | [-0.234, 0.379] | [-0.399, 0.403] | [-0.259, 0.406] | ✗ |
| α -TOST | [-0.034, 0.229] | [0.005, 0.141] | [-0.087, 0.091] | [0.001, 0.147] | ✗ |
| cTOST | [0.012, 0.184] | [-0.027, 0.172] | [-0.101, 0.106] | [-0.029, 0.175] | ✓ |

Table 1: Confidence intervals obtained using the multivariate TOST, α -TOST, and cTOST for the four-dimensional case study related to econazole nitrate deposition in porcine skin. The rejection region is $(-c_0, c_0)$ with $c_0 = \log(1.25) \approx 0.223$ and the nominal significance level is $\alpha_0 = 5\%$. Bioequivalence is declared by a method when all intervals are within $(-c_0, c_0)$.

protocol, leading to $\nu_1 = 12$ and $\nu_2 = 11$. Measurements at 21 different skin depths recorded in [Quartier et al. \(2019\)](#) were grouped to obtain $K = 4$ anatomically relevant regions: *stratum corneum* (0–20 μm ; $\hat{\theta}_1 \approx 0.0976$, $\hat{\sigma}_{1,1} \approx 0.3305$), *viable epidermis* (20–160 μm ; $\hat{\theta}_2 \approx 0.0726$, $\hat{\sigma}_{1,2} \approx 0.1708$), *upper dermis* (160–400 μm ; $\hat{\theta}_3 \approx 0.0022$, $\hat{\sigma}_{1,3} \approx 0.2233$) and *lower dermis* (400–800 μm ; $\hat{\theta}_4 \approx 0.0733$, $\hat{\sigma}_{1,4} \approx 0.1853$).

The results of multivariate bioequivalence assessment using the multivariate TOST, multivariate α -TOST, and multivariate cTOST are presented in Table 1. As customary in this literature, we set $c_0 = \log(1.25)$ and $\alpha_0 = 5\%$. Based on the conservative behavior of multivariate cTOST reported in an emulation study based on these data (not provided here), no further refinement was pursued. We present marginal confidence intervals for each of the four biodistribution profiles, as well as an indication of whether the test procedure declares bioequivalence (i.e., whether each marginal confidence interval is contained in the equivalence margins according to the IIP). Since $c_0 > \hat{c}_k^*$ for all $k = 1, \dots, K$, cTOST also allows for an IIP-based interpretation by considering the intervals $\hat{\theta}_k \pm \{c_0 - \hat{c}_k^*\}$ (see Appendix J). Both the multivariate

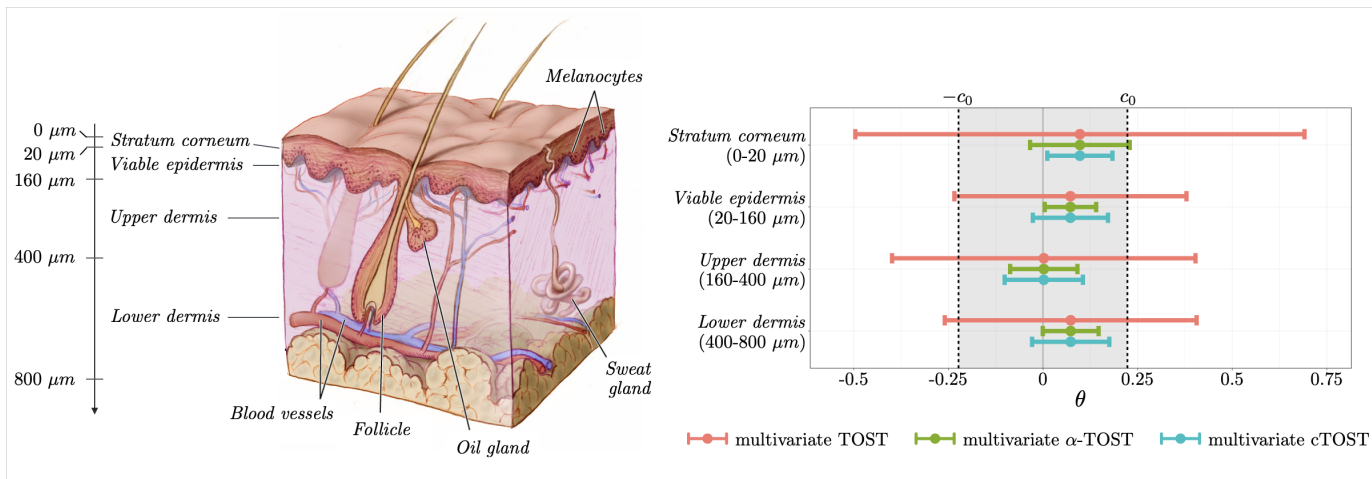


Figure 3: Left: cross-sectional diagram of the skin highlighting its key structures. Right: Representation of the confidence intervals obtained by the multivariate TOST, α -TOST, and cTOST as reported in Table 1 for the four-dimensional case study related to econazole nitrate deposition in porcine skin. Bioequivalence is declared by a method when all intervals are within $(-c_0, c_0)$.

TOST and multivariate α -TOST fail to declare bioequivalence in the considered application. In contrast, the multivariate cTOST detects bioequivalence between the two topical formulations. This distinction is further illustrated in Figure 3, which depicts the bioequivalence assessment problem in terms of equivalence margins and marginal confidence intervals. In particular, while the TOST becomes extremely conservative, the α -TOST leads to an improvement in terms of power by producing shorter confidence intervals. However, the α -TOST suffers not only from its marginal lack of power compared to the cTOST but also as it corrects all dimensions in the same manner. Instead, the cTOST leads to more balanced rejection regions as highlighted by the length of its confidence intervals, where its longest confidence interval remains shorter than the ones provided by competing methods.

6 Final Remarks

In this article, we presented a novel cTOST procedure in the context of multivariate average equivalence testing. The univariate cTOST is the uniformly most powerful test under known variance, and remains the optimal adjustment when the variance is estimated. In small samples, we propose a refinement for cTOST, which can be computed easily, and can ensure that the test size remains close to the nominal significance level. The univariate refinement similarly applies to the multivariate setting. We find the multivariate setting much more complex, with no single adjustment remaining uniformly more powerful over the entire alternative space even under a known covariance structure. To complicate matters further, for any fixed parameter vector in the alternative space, the most powerful adjustments often correspond to rejection regions that are highly unbalanced across the K dimensions (i.e., marginal rejection regions close to zero in some dimensions and potentially unbounded for others), failing to reflect the practical situations of interest to scientists. Therefore, we constrain the marginal size of each univariate test to a constant and propose multivariate cTOST, which retains certain optimality, is computationally simple, and yields rejection regions that align with practical needs in scientific applications.

By improving the efficiency and reliability of bioequivalence studies, which play a pivotal role in biopharmaceutical development ([Patterson and Jones 2017](#)), the cTOST method can facilitate the approval process for generic medical products.

This is particularly important for locally acting drugs, where current methodological constraints often limit the development of generic products (Miranda et al. 2018a,b). These advancements align with the World Health Organization’s goal of ensuring access to safe, effective, high-quality, and affordable medicines, advancing the vision of Universal Health Coverage, particularly in low- and middle-income countries where affordability and availability remain key obstacles (Wirtz et al. 2017). The broad applicability of our methodology extends beyond traditional bioequivalence studies to general equivalence tests across various disciplines (Lakens et al. 2018, Moore et al. 2022, Aggarwal et al. 2023). The cTOST method specifically addresses common challenges across these domains, such as reduced sample sizes and/or the presence of multivariate outcome measures. By achieving larger power while maintaining type I error rates, cTOST provides practical solutions for researchers and practitioners across different fields.

References

- Aggarwal, M., J. Allen, A. Coppock, D. Frankowski, S. Messing, K. Zhang, J. Barnes, A. Beasley, H. Hantman, and S. Zheng (2023). A 2 million-person, campaign-wide field experiment shows how digital advertising affects voter turnout. Nature Human Behaviour 7, 332–341.
- Anderson, S. and W. W. Hauck (1983). A new procedure for testing equivalence in comparative bioavailability and other clinical trials. Communications in Statistics-Theory and Methods 12(23), 2663–2692.
- Babiskin, A., F. Wu, Y. Mousa, M.-L. Tan, E. Tsakalozou, R. L. Walenga, M. Yoon, S. G. Raney, J. E. Polli, A. Schwendeman, et al. (2023). Regulatory utility of mechanistic

- modeling to support alternative bioequivalence approaches: a workshop overview. CPT: Pharmacometrics & Systems Pharmacology 12(5), 619–623.
- Berger, R. L. (1982). Multiparameter hypothesis testing and acceptance sampling. Technometrics 24(4), 295–300.
- Berger, R. L. and J. C. Hsu (1996). Bioequivalence trials, intersection-union tests and equivalence confidence sets. Statistical Science 11, 283–319.
- Boulaguiem, Y., L. Insolia, M.-P. Victoria-Feser, D.-L. Couturier, and S. Guerrier (2025). Multivariate adjustments for average equivalence testing. Statistics in Medicine 44(15-17), e10258.
- Boulaguiem, Y., J. Quartier, M. Lapteva, Y. N. Kalia, M.-P. Victoria-Feser, S. Guerrier, and D.-L. Couturier (2024). Finite sample corrections for average equivalence testing. Statistics in Medicine 43(5), 833–854.
- Chervoneva, I., T. Hyslop, and W. W. Hauck (2007). A multivariate test for population bioequivalence. Statistics in Medicine 26(6), 1208–1223.
- Cordery, S., A. Pensado, W. Chiu, M. Shehab, A. Bunge, M. Delgado-Charro, and R. Guy (2017). Topical bioavailability of diclofenac from locally-acting, dermatological formulations. International Journal of Pharmaceutics 529(1-2), 55–64.
- Counsell, A. and R. A. Cribbie (2015). Equivalence tests for comparing correlation and regression coefficients. British Journal of Mathematical and Statistical Psychology 68(2), 292–309.
- Davit, B. M., M.-L. Chen, D. P. Conner, S. H. Haidar, S. Kim, C. H. Lee, R. A. Lionberger, F. T. Makhlouf, P. E. Nwakama, D. T. Patel, et al. (2012). Implementation of a reference-scaled average bioequivalence approach for highly variable generic drug products by the us food and drug administration. The AAPS journal 14, 915–924.
- Deng, Y. and X.-H. Zhou (2020). Methods to control the empirical type I error rate in average bioequivalence tests for highly variable drugs. Statistical Methods in Medical Research 29, 1650–1667.
- Dolado, J. J., M. C. Otero, and M. Harman (2014). Equivalence hypothesis testing in experimental software engineering. Software Quality Journal 22(2), 215–238.
- Du, L. and L. Choi (2015). Likelihood approach for evaluating bioequivalence of highly variable drugs. Pharmaceutical Statistics 14(2), 82–94.
- EMA (2018, October). Draft guideline on quality and equivalence of topical products. Accessed on: 2024-05-31.

- FDA (2022, October). Physicochemical and Structural (Q3) Characterization of Topical Drug Products Submitted in ANDAs. Guidance for Industry. Accessed on: 2024-05-31.
- Herkenne, C., I. Alberti, A. Naik, Y. N. Kalia, F.-X. Mathy, V. Pr eat, and R. H. Guy (2008). In vivo methods for the assessment of topical drug bioavailability. Pharmaceutical Research *25*, 87–103.
- Jones, B. and M. G. Kenward (2003). Design and Analysis of Cross-Over Trials (3rd ed.). London: Chapman and Hall/CRC.
- Labes, D. and H. Sch utz (2016). Inflation of type I error in the evaluation of scaled average bioequivalence, and a method for its control. Pharmaceutical Research *33*, 2805–2814.
- Lakens, D., A. M. Scheel, and P. M. Isager (2018). Equivalence testing for psychological research: A tutorial. Advances in Methods and Practices in Psychological Science *1*, 259–269.
- Lehmann, E. L. (1986). Testing Statistical Hypothesis (2nd ed.). New York: Wiley.
- Li, B. and G. J. Babu (2019). A graduate Course on Statistical Inference. New York: Springer.
- Lukic, M., I. Pantelic, and S. Savic (2020). A comparison of myribase and doublebase gel: Does qualitative similarity of emollient products imply their direct interchangeability in everyday practice? Dermatologic Therapy *33*(6), e14020.
- Mehta, M., B. Schug, H. Blume, G. Beuerle, W. Jiang, J. Koenig, P. Paixao, N. Tampal, Y.-C. Tsang, J. Walstab, et al. (2023). The global bioequivalence harmonisation initiative (GBHI): Report of the fifth international EUFEPS/AAPS conference. European Journal of Pharmaceutical Sciences *190*, 106566.
- Meyners, M. (2012). Equivalence tests – A review. Food Quality and Preference *26*, 231–245.
- Miranda, M., J. J. Sousa, F. Veiga, C. Cardoso, and C. Vitorino (2018a). Bioequivalence of topical generic products. Part 1: Where are we now? European Journal of Pharmaceutical Sciences *123*, 260–267.
- Miranda, M., J. J. Sousa, F. Veiga, C. Cardoso, and C. Vitorino (2018b). Bioequivalence of topical generic products. Part 2. Paving the way to a tailored regulatory system. European Journal of Pharmaceutical Sciences *122*, 264–272.
- Miranda, M., C. Veloso, M. Brown, A. A. Pais, C. Cardoso, and C. Vitorino (2022). Topical bioequivalence: Experimental and regulatory considerations following formulation complexity. International Journal of Pharmaceutics *620*, 121705.

- Moore, N., R. Steger, B. Bowers, and A. Taylor (2022). Investigation of IDEAL-CT device equivalence: Are all devices equal? Transportation Research Record 2676(5), 1–12.
- Muñoz, J., D. Alcaide, and J. Ocaña (2016). Consumer’s risk in the EMA and FDA regulatory approaches for bioequivalence in highly variable drugs. Statistics in Medicine 35(12), 1933–1943.
- Ocaña, J. and J. Muñoz (2019). Controlling type I error in the reference-scaled bioequivalence evaluation of highly variable drugs. Pharmaceutical Statistics 18(5), 583–599.
- Pallmann, P. and T. Jaki (2017). Simultaneous confidence regions for multivariate bioequivalence. Statistics in Medicine 36(29), 4585–4603.
- Patil, P. P., A. P. Pawar, K. R. Mahadik, and V. L. Gaikwad (2021). An overview of regulations for bioequivalence assessment of locally acting orally inhaled drug products for the united states, europe, canada, and india. Expert Opinion on Drug Delivery 18(12), 1843–1855.
- Patterson, S. D. and B. Jones (2017). Bioequivalence and Statistics in Clinical Pharmacology (2nd ed.). New York: Chapman and Hall/CRC.
- Phillips, K. F. (2009). Power for testing multiple instances of the two one-sided tests procedure. The International Journal of Biostatistics 5(1), 1–12.
- Quartier, J., N. Capony, M. Lapteva, and Y. N. Kalia (2019). Cutaneous biodistribution: A high-resolution methodology to assess bioequivalence in topical skin delivery. Pharmaceutics 11, 484.
- Romano, J. P. (2005). Optimal testing of equivalence hypotheses. The Annals of Statistics 33(3), 1036 – 1047.
- Schuirman, D. J. (1987). A comparison of the two one-sided tests procedure and the power approach for assessing the equivalence of average bioavailability. Journal of Pharmacokinetics and Biopharmaceutics 15(6), 657–680.
- Schütz, H., D. Labes, and M. J. Wolfsegger (2022). Critical remarks on reference-scaled average bioequivalence. Journal of Pharmacy & Pharmaceutical Sciences 25, 285–296.
- Shin, S. H., E. Rantou, S. G. Raney, P. Ghosh, H. Hassan, and A. Stinchcomb (2020). Cutaneous pharmacokinetics of acyclovir cream 5% products: Evaluating bioequivalence with an in vitro permeation test and an adaptation of scaled average bioequivalence. Pharmaceutical Research 37, 1–13.

- Tothfalusi, L., L. Endrenyi, and A. G. Arieta (2009). Evaluation of bioequivalence for highly variable drugs with scaled average bioequivalence. Clinical Pharmacokinetics 48, 725–743.
- Tseng, Y.-L. (2002). Optimal confidence sets for testing average bioequivalence. Test 11(1), 127–141.
- Volontè, P., U. M. Musazzi, L. Arnaboldi, M. A. Ortenzi, A. Casiraghi, F. Cilurzo, and P. Minghetti (2024). Equivalence assessment of creams with quali-quantitative differences in light of the EMA and FDA regulatory framework. European Journal of Pharmaceutical Sciences 195, 106726.
- Wang, W., J. Gene Hwang, and A. Dasgupta (1999). Statistical tests for multivariate bioequivalence. Biometrika 86(2), 395–402.
- Wellek, S. (2010). Testing Statistical Hypotheses of Equivalence and Noninferiority (2nd ed.). New York: Chapman and Hall/CRC.
- Wirtz, V. J., H. V. Hogerzeil, A. L. Gray, M. Bigdeli, C. P. de Joncheere, M. A. Ewen, M. Gyansa-Lutterodt, S. Jing, V. L. Luiza, R. M. Mbindyo, et al. (2017). Essential medicines for universal health coverage. The Lancet 389(10067), 403–476.

SUPPLEMENTARY MATERIAL

A Equivalence of all adjustments in $\mathcal{A}(\alpha_0)$ when σ_1 is known

When σ_1 is known, the canonical form of the univariate average equivalence problem described in (2) for $K = 1$ reduces to

$$\hat{\theta} \sim \mathcal{N}(\theta, \sigma_1^2).$$

The TOST is thus based on the two following test statistics:

$$Z_L \equiv \frac{\hat{\theta} + c}{\sigma_1} \quad \text{and} \quad Z_U \equiv \frac{\hat{\theta} - c}{\sigma_1},$$

where Z_L tests for $H_{01} : \theta \leq -c$ versus $H_{11} : \theta > -c$, and Z_U tests for $H_{02} : \theta \geq c$ versus $H_{12} : \theta < c$. At a significance level α , we reject $H_0 \equiv H_{01} \cup H_{02}$ in favor of $H_1 \equiv H_{11} \cap H_{12}$ if both tests simultaneously reject their marginal null hypotheses, that is, if

$$Z_L \geq z_\alpha \quad \text{and} \quad Z_U \leq -z_\alpha,$$

where z_α denotes the upper α quantile of a normal distribution. Using $\omega(c_0, \sigma_1, \nu_2, 0, c)$ defined after (7) and letting the size of the test to be α_0 , we have

$$\omega(c_0, \sigma_1, \infty, z_\alpha, c) = \Phi\left(\frac{c - c_0}{\sigma_1} - z_\alpha\right) - \Phi\left(-\frac{c + c_0}{\sigma_1} + z_\alpha\right) = \alpha_0.$$

This allows us to determine a unique $c(z_\alpha)$ for any subjectively selected z_α , i.e., for any $z \geq 0$, $c(z)$ is such that

$$\omega\{c_0, \sigma_1, \infty, z, c(z)\} = \Phi\left\{\frac{c(z) - c_0}{\sigma_1} - z\right\} - \Phi\left\{-\frac{c(z) + c_0}{\sigma_1} + z\right\} = \alpha_0.$$

The power of such a test is

$$\omega\{\theta, \sigma_1, \infty, z, c(z)\} = \Phi\left\{\frac{c(z) - \theta}{\sigma_1} - z\right\} - \Phi\left\{-\frac{c(z) + \theta}{\sigma_1} + z\right\}.$$

Because

$$\alpha_0 = \Phi\left[-\frac{c_0}{\sigma_1} + \left\{\frac{c(z)}{\sigma_1} - z\right\}\right] - \Phi\left[-\frac{c_0}{\sigma_1} - \left\{\frac{c(z)}{\sigma_1} - z\right\}\right],$$

hence $\frac{c(z)}{\sigma_1} - z$ is unique regardless of the choice of z . Thus,

$$\omega\{\theta, \sigma_1, z, \infty, c(z)\} = \Phi\left[-\frac{\theta}{\sigma_1} + \left\{\frac{c(z)}{\sigma_1} - z\right\}\right] - \Phi\left[-\frac{\theta}{\sigma_1} - \left\{\frac{c(z)}{\sigma_1} - z\right\}\right],$$

does not change as z changes. This means regardless of the choice of z , any test at size α_0 has the same power.

As an illustration, Figure A.1 compares the power at $\theta = 0$ as a function of α in both the unknown and known σ_1 cases. We set $\sigma_1 = 0.1$, $\nu_2 = 15$, $c_0 = \log(1.25)$, and $\alpha_0 = 0.05$. The pink curve represents the power $\omega\{\theta, \sigma_1, \nu_2, \alpha, \nu_2, c(t_{\alpha, \nu_2}, \nu_2)\}$ when σ_1 is unknown. This curve is upper bounded by the constant blue line, which represents the power when σ_1 is known. The dashed vertical lines correspond to values of α associated with the δ -TOST, α -TOST, and cTOST, respectively. This shows that setting α to $1/2$ results in the most powerful adjustment when σ_1 is unknown.

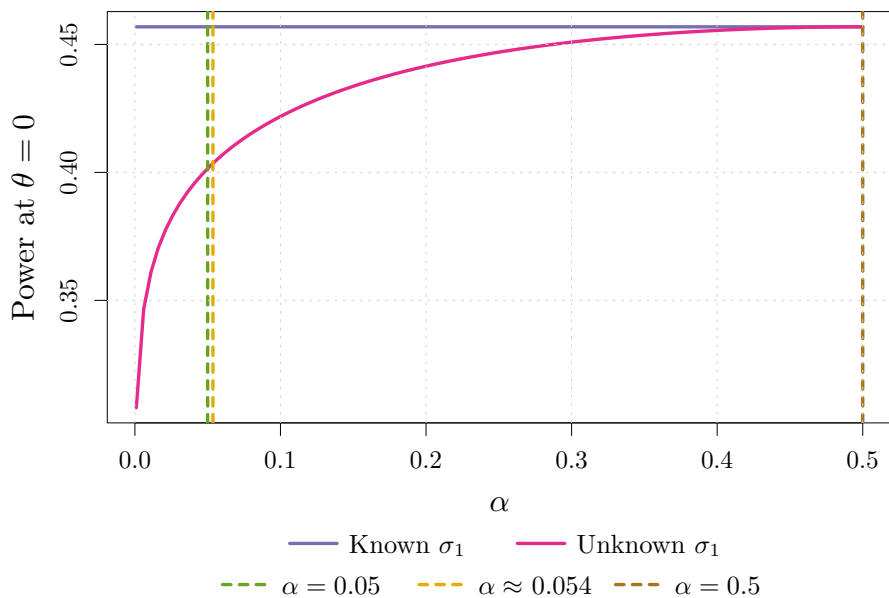


Figure A.1: Power of adjusted TOST procedures at $\theta = 0$ as a function of α when σ_1 is known (flat blue line) and unknown (increasing pink curve). Dashed vertical lines represent the increasing α values associated to the δ -TOST ($\alpha = 0.05$), α -TOST ($\alpha = 0.054$), and cTOST ($\alpha = 0.5$), respectively.

B Proof of Theorem 1

Consider the test

$$H_0 : \mu \geq c_0/\sigma_1 \text{ or } \mu \leq -c_0/\sigma_1, \quad H_1 : -c_0/\sigma_1 < \mu < c_0/\sigma_1,$$

using a single observation $X = \hat{\theta}/\sigma_1 \sim N(\mu, 1)$ with known σ_1 . Below, we use Theorem 3.5 in [Li and Babu \(2019\)](#) to prove that the test with rejection region $(-c(0)/\sigma_1, c(0)/\sigma_1)$ is the most powerful test at level α_0 in this case. Define the decision function $\tilde{\phi}(X) = 1$ if $X \in (-c(0)/\sigma_1, c(0)/\sigma_1)$ and $\tilde{\phi}(X) = 0$ if $X \in (\infty, -c(0)/\sigma_1] \cup [c(0)/\sigma_1, \infty)$. Then we can check that $\tilde{\phi}(X)$ satisfies Lemma 3.9 when we set $f(x)$ to be the normal pdf with mean $-c_0/\sigma_1$ and variance 1, $h(x)$ to be the normal pdf with mean c_0/σ_1 and variance 1, $Y(x) = x$, $t_1 = -c(0)/\sigma_1$, $t_2 = c(0)/\sigma_1$, $\gamma_1 = \gamma_2 = 0$, and $\alpha = \alpha_0$. In particular, we can verify that

$$E_{\mu=-c_0/\sigma_1} \tilde{\phi}(X) = \Phi\left(\frac{c(0) + c_0}{\sigma_1}\right) - \Phi\left(\frac{-c(0) + c_0}{\sigma_1}\right) = \alpha_0$$

due to the definition of $c(0)$. Likewise,

$$\begin{aligned}
E_{\mu=c_0/\sigma_1} \tilde{\phi}(X) &= \Phi\left(\frac{c(0) - c_0}{\sigma_1}\right) - \Phi\left(\frac{-c(0) - c_0}{\sigma_1}\right) \\
&= \Phi\left(\frac{c(0) + c_0}{\sigma_1}\right) - \Phi\left(\frac{-c(0) + c_0}{\sigma_1}\right) \\
&= \alpha_0.
\end{aligned}$$

Now result (2) in Theorem 3.5 implies the test is the most powerful, where the power at θ/σ_1 is

$$\Phi\left(\frac{c(0) + \theta}{\sigma_1}\right) - \Phi\left(\frac{-c(0) + \theta}{\sigma_1}\right) = \omega\{\theta, \sigma_1, \infty, 0, c(0)\}.$$

Now consider the test of the same hypotheses with rejection region

$$\hat{\theta}/\sigma_1 \in (t - c(t, \nu_2)/\sigma_1, c(t, \nu_2)/\sigma_1 - t),$$

where $c(t, \nu_2)$ satisfies

$$\omega\{c_0, \sigma_1, \nu_2, t, c(t, \nu_2)\} = \alpha_0.$$

This is a test with the same level, hence it is less powerful, thus, $\omega(\theta, \sigma_1, \nu_2, t, c(t, \nu_2)) \leq \omega\{\theta, \sigma_1, \infty, 0, c(0)\} = \omega\{\theta, \sigma_1, \nu_2, 0, c(0)\}$. \square

C Proof of Proposition 1

Proof of result 1 from Proposition 1. First of all, $\nu_2 \widehat{\sigma}^2 / \sigma^2$ has a chi-squared distribution with mean ν_2 , variance $2\nu_2$, hence $\widehat{\sigma}^2 / \sigma^2 = 1 + O_p(\nu_2^{-1/2})$, thus $\widehat{\sigma}_1 / \sigma_1 = 1 + O_p(\nu_2^{-1/2})$. Next, from $\Phi\left(\frac{c_0 + c(0)}{\sigma_1}\right) - \Phi\left(\frac{c_0 - c(0)}{\sigma_1}\right) = \alpha_0$ and $\{c_0 + c(0)\} / \sigma_1 \rightarrow \infty$, we have $c(0) < c_0$ for sufficiently large ν_1 . For sufficiently large ν_1 , we have

$$1 - \alpha_0 > \Phi\left(\frac{c_0 - c(0)}{\sigma_1}\right) = \Phi\left(\frac{c_0 + c(0)}{\sigma_1}\right) - \alpha_0 > 1 - 2\alpha_0,$$

thus, $0 < \{c_0 - c(0)\} / \sigma_1 \asymp 1$. This implies

$$c_1 \sigma_1 < c(0) - c_0 < c_2 \sigma_1, \tag{A.1}$$

where $c_1 \equiv \Phi^{-1}(1 - \alpha_0)$, $c_2 \equiv \Phi^{-1}(1 - 2\alpha_0)$ are two positive constants.

From a Taylor expansion, we get

$$\begin{aligned}
\alpha_0 &= \Phi\left(\frac{c_0 + \widehat{c}(0)}{\widehat{\sigma}_1}\right) - \Phi\left(\frac{c_0 - \widehat{c}(0)}{\widehat{\sigma}_1}\right) \\
&= \Phi\left(\frac{c_0 + c(0)}{\sigma_1}\right) - \Phi\left(\frac{c_0 - c(0)}{\sigma_1}\right) \\
&\quad + \left\{ \phi\left(\frac{c_0 + c(0)}{\sigma_1}\right) + \phi\left(\frac{c(0) - c_0}{\sigma_1}\right) \right\} \frac{\widehat{c}(0) - c(0)}{\sigma_1} \\
&\quad - \left\{ \phi\left(\frac{c_0 + c(0)}{\sigma_1}\right) \frac{c(0) + c_0}{\sigma_1} + \phi\left(\frac{c(0) - c_0}{\sigma_1}\right) \frac{c(0) - c_0}{\sigma_1} \right\} \frac{\widehat{\sigma}_1 - \sigma_1}{\sigma_1} + r_1 \\
&= \alpha_0 + \phi\left(\frac{c(0) - c_0}{\sigma_1}\right) \frac{\widehat{c}(0) - c(0)}{\sigma_1} - \phi\left(\frac{c(0) - c_0}{\sigma_1}\right) \frac{c(0) - c_0}{\sigma_1} \frac{\widehat{\sigma}_1 - \sigma_1}{\sigma_1} + r_2 \\
&= \alpha_0 + \phi\left(\frac{c(0) - c_0}{\sigma_1}\right) \frac{\widehat{c}(0) - c(0)}{\sigma_1} + O_p(\nu_2^{-1/2}),
\end{aligned}$$

where r_1, r_2 are the residual terms that are of higher order. This leads to $\widehat{c}(0) - c(0) = O_p(\sigma_1 \nu_2^{-1/2})$. This in combination with $c(0) = c_0 + O_p(\sigma_1) \asymp 1$ leads to $\widehat{c}(0) - c(0) = o_p\{c(0)\}$. \square

Proof of result 2 from Proposition 1. First, from

$$\begin{aligned}
\alpha_0 &= \int_0^{c(t, \nu_2)/t} \left[\Phi\left(\frac{c_0 + c(t, \nu_2) - xt}{\sigma_1}\right) - \Phi\left(\frac{c_0 - c(t, \nu_2) + xt}{\sigma_1}\right) \right] f_W(x|\sigma_1, \nu_2) dx \\
&< \int_0^\infty \left[\Phi\left(\frac{c_0 + c(t, \nu_2) - xt}{\sigma_1}\right) - \Phi\left(\frac{c_0 - c(t, \nu_2) + xt}{\sigma_1}\right) \right] f_W(x|\sigma_1, \nu_2) dx \\
&< 1 - \Phi\left(\frac{c_0 - c(t, \nu_2)}{\sigma_1}\right),
\end{aligned}$$

$\{c_0 - c(t, \nu_2)\}/\sigma_1 \leq c_1$. Thus, $c(t, \nu_2)/\sigma_1 \geq c_0/\sigma_1 - c_1 \rightarrow \infty$. On the other hand,

$$\begin{aligned}
\alpha_0 &= \int_0^{c(t, \nu_2)/t} \left[\Phi \left(\frac{c_0 + c(t, \nu_2) - xt}{\sigma_1} \right) - \Phi \left(\frac{c_0 - c(t, \nu_2) + xt}{\sigma_1} \right) \right] f_W(x|\sigma_1, \nu_2) dx \\
&> \int_0^{c(t, \nu_2)/t} \left[\Phi \left(\frac{c_0}{\sigma_1} \right) - \Phi \left(\frac{c_0 - c(t, \nu_2) + xt}{\sigma_1} \right) \right] f_W(x|\sigma_1, \nu_2) dx \\
&= \Phi \left(\frac{c_0}{\sigma_1} \right) \int_0^{c(t, \nu_2)/t} f_W(x|\sigma_1, \nu_2) dx - \int_0^{c(t, \nu_2)/t} \Phi \left(\frac{c_0 - c(t, \nu_2) + xt}{\sigma_1} \right) f_W(x|\sigma_1, \nu_2) dx \\
&= \Phi \left(\frac{c_0}{\sigma_1} \right) \int_0^{\{c(t, \nu_2)/(t\sigma_1)\}^2} g(y, \nu_2) dy - \int_0^{\{c(t, \nu_2)/(t\sigma_1)\}^2} \Phi \left(\frac{c_0 - c(t, \nu_2)}{\sigma_1} + \sqrt{yt} \right) g(y, \nu_2) dy,
\end{aligned}$$

where

$$g(y, \nu_2) = \frac{(\nu_2 y)^{\nu_2/2-1} e^{-\nu_2 y/2}}{2^{\nu_2/2} \Gamma(\frac{\nu_2}{2})} \nu_2.$$

Note that $g(y, \nu_2)$ has mean 1 and variance $2/\nu_2$, hence

$$\begin{aligned}
&\int_0^{\{c(t, \nu_2)/(t\sigma_1)\}^2} \Phi \left(\frac{c_0 - c(t, \nu_2)}{\sigma_1} + \sqrt{yt} \right) g(y, \nu_2) dy \\
&> \Phi \left(\frac{c_0}{\sigma_1} \right) \int_0^{\{c(t, \nu_2)/(t\sigma_1)\}^2} g(y, \nu_2) dy - \alpha_0 \\
&\rightarrow 1 - \alpha_0
\end{aligned}$$

when $\nu_1, \nu_2 \rightarrow \infty$, hence for ν_1, ν_2 sufficiently large,

$$\begin{aligned} & \int_0^{1+\nu_2^{-1/3}} \Phi \left(\frac{c_0 - c(t, \nu_2)}{\sigma_1} + \sqrt{yt} \right) g(y, \nu_2) dy \\ & + \int_{1+\nu_2^{-1/3}}^{\{c(t, \nu_2)/(t\sigma_1)\}^2} \Phi \left(\frac{c_0 - c(t, \nu_2)}{\sigma_1} + \sqrt{yt} \right) g(y, \nu_2) dy > 1 - 1.5\alpha_0. \end{aligned}$$

Now

$$\begin{aligned} & \int_{1+\nu_2^{-1/3}}^{\{c(t, \nu_2)/(t\sigma_1)\}^2} \Phi \left(\frac{c_0 - c(t, \nu_2)}{\sigma_1} + \sqrt{yt} \right) g(y, \nu_2) dy \\ & \leq \int_{1+\nu_2^{-1/3}}^{\{c(t, \nu_2)/(t\sigma_1)\}^2} g(y, \nu_2) dy \\ & \rightarrow 0 \end{aligned}$$

when $\nu_2 \rightarrow \infty$, hence

$$\Phi \left(\frac{c_0 - c(t, \nu_2)}{\sigma_1} + (1 + \nu_2^{-1/3})t \right) \geq \int_0^{1+\nu_2^{-1/3}} \Phi \left(\frac{c_0 - c(t, \nu_2)}{\sigma_1} + \sqrt{yt} \right) g(y, \nu_2) dy > 1 - 2\alpha_0$$

for sufficiently large ν_1, ν_2 . This implies $\{c_0 - c(t, \nu_2)\}/\sigma_1 \geq c_2 - (1 + \nu_2^{-1/3})t$. We

thus obtain

$$c_2 - (1 + \nu_2^{-1/3})t \leq \{c_0 - c(t, \nu_2)\}/\sigma_1 \leq c_1, \quad (\text{A.2})$$

hence $|c_0 - c(t, \nu_2)| = O(\sigma_1)$. This leads to $c(t, \nu_2) = c_0 + O(\sigma_1) = c_0 + o(1)$ and

hence $c(t, \nu_2)/t \asymp 1$.

From a Taylor expansion, we get

$$\begin{aligned}
\alpha_0 &= \int_0^{\widehat{c}(t, \nu_2)/t} \left[\Phi \left(\frac{c_0 + \widehat{c}(t, \nu_2) - xt}{\widehat{\sigma}_1} \right) + \Phi \left(\frac{\widehat{c}(t, \nu_2) - c_0 - xt}{\widehat{\sigma}_1} \right) - 1 \right] f_W(x|\sigma_1, \nu_2) dx \\
&= \int_0^{c(t, \nu_2)/t} \left[\Phi \left(\frac{c_0 + c(t, \nu_2) - xt}{\sigma_1} \right) + \Phi \left(\frac{c(t, \nu_2) - c_0 - xt}{\sigma_1} \right) - 1 \right] f_W(x|\sigma_1, \nu_2) dx \\
&\quad + \frac{\widehat{c}(t, \nu_2) - c(t, \nu_2)}{\sigma_1} \int_0^{c(t, \nu_2)/t} \left[\phi \left(\frac{c_0 + c(t, \nu_2) - xt}{\sigma_1} \right) \right. \\
&\quad \left. + \phi \left(\frac{c(t, \nu_2) - c_0 - xt}{\sigma_1} \right) \right] f_W(x|\sigma_1, \nu_2) dx \\
&\quad - \frac{\widehat{\sigma}_1 - \sigma_1}{\sigma_1} \int_0^{c(t, \nu_2)/t} \left[\phi \left(\frac{c_0 + c(t, \nu_2) - xt}{\sigma_1} \right) \frac{c_0 + c(t, \nu_2) - xt}{\sigma_1} \right. \\
&\quad \left. + \phi \left(\frac{c(t, \nu_2) - c_0 - xt}{\sigma_1} \right) \frac{c(t, \nu_2) - c_0 - xt}{\sigma_1} \right] f_W(x|\sigma_1, \nu_2) dx + r_1 \\
&= \alpha_0 + \frac{\widehat{c}(t, \nu_2) - c(t, \nu_2)}{\sigma_1} \int_0^{c(t, \nu_2)/t} \phi \left(\frac{c(t, \nu_2) - c_0 - xt}{\sigma_1} \right) f_W(x|\sigma_1, \nu_2) dx \\
&\quad - \frac{\widehat{\sigma}_1 - \sigma_1}{\sigma_1} \int_0^{c(t, \nu_2)/t} \phi \left(\frac{c(t, \nu_2) - c_0 - xt}{\sigma_1} \right) \frac{c(t, \nu_2) - c_0 - xt}{\sigma_1} f_W(x|\sigma_1, \nu_2) dx + r_2.
\end{aligned}$$

Here we note that both integrals above are bounded, and r_1, r_2 are higher order terms that are ignorable. Thus,

$$\begin{aligned}
&|\widehat{c}(t, \nu_2) - c(t, \nu_2)| \\
&\leq 2\sigma_1 \frac{\frac{|\widehat{\sigma}_1 - \sigma_1|}{\sigma_1} \left| \int_0^{c(t, \nu_2)/t} \phi \left(\frac{c_0 - c(t, \nu_2) + xt}{\sigma_1} \right) \frac{c_0 - c(t, \nu_2) + xt}{\sigma_1} f_W(x|\sigma_1, \nu_2) dx \right|}{\int_0^{c(t, \nu_2)/t} \phi \left(\frac{c(t, \nu_2) - c_0 - xt}{\sigma_1} \right) f_W(x|\sigma_1, \nu_2) dx} \\
&= O_p(\sigma_1 \nu_2^{-1/2}) \frac{\left| \int_0^{\{c(t, \nu_2)/(t\sigma_1)\}^2} \phi \left(\frac{c_0 - c(t, \nu_2)}{\sigma_1} + \sqrt{yt} \right) \left(\frac{c_0 - c(t, \nu_2)}{\sigma_1} + \sqrt{yt} \right) g(y, \nu_2) dy \right|}{\int_0^{\{c(t, \nu_2)/(t\sigma_1)\}^2} \phi \left(\frac{c_0 - c(t, \nu_2)}{\sigma_1} + \sqrt{yt} \right) g(y, \nu_2) dy}.
\end{aligned}$$

Note that

$$\begin{aligned}
& \lim_{\nu_1, \nu_2 \rightarrow \infty} \frac{\left| \int_0^{\{c(t, \nu_2)/(t\sigma_1)\}^2} \phi\left(\frac{c_0 - c(t, \nu_2)}{\sigma_1} + \sqrt{yt}\right) \left(\frac{c_0 - c(t, \nu_2)}{\sigma_1} + \sqrt{yt}\right) g(y, \nu_2) dy \right|}{\int_0^{\{c(t, \nu_2)/(t\sigma_1)\}^2} \phi\left(\frac{c_0 - c(t, \nu_2)}{\sigma_1} + \sqrt{yt}\right) g(y, \nu_2) dy} \\
&= \lim_{\nu_1, \nu_2 \rightarrow \infty} \frac{\left| \phi\left(\frac{c_0 - c(t, \nu_2)}{\sigma_1} + t\right) \left(\frac{c_0 - c(t, \nu_2)}{\sigma_1} + t\right) \right|}{\phi\left(\frac{c_0 - c(t, \nu_2)}{\sigma_1} + t\right)} \\
&= \lim_{\nu_1, \nu_2 \rightarrow \infty} \left| \frac{c_0 - c(t, \nu_2)}{\sigma_1} + t \right| \\
&= O(1).
\end{aligned}$$

Thus,

$$\widehat{c}(t, \nu_2) - c(t, \nu_2) = O_p(\sigma_1 \nu_2^{-1/2}).$$

We also have $c(t, \nu_2) - t\widehat{\sigma}_1 = c(t, \nu_2) - t\sigma_1 + O_p(\sigma_1/\sqrt{\nu_2}) = c_0 - t\sigma_1 + O_p(\sigma_1 + \sigma_1/\sqrt{\nu_2}) = c_0 + o_p(1)$. Thus we indeed have

$$\widehat{c}(t, \nu_2) - c(t, \nu_2) = o_p\{c(t, \nu_2) - t\widehat{\sigma}_1\}.$$

□

Proof of result 3 from Proposition 1. The rejection region at $t = 0$ is $C\{0, c(0)\} = \{\widehat{\theta} : -c(0) < \widehat{\theta} < c(0)\}$, while when $t \neq 0$, the rejection region is $C\{t, c(t)\} = \{\widehat{\theta} : t\widehat{\sigma}_1 - c(t, \nu_2) < \widehat{\theta} < c(t, \nu_2) - t\widehat{\sigma}_1\}$. Note that the approximation errors of the two

approximate rejections are both $\widehat{c}(0) - c(0) = O_p(\sigma_1 \nu_2^{-1/2})$ and $\widehat{c}(t, \nu_2) - c(t, \nu_2) = O_p(\sigma_1 \nu_2^{-1/2})$. Now we have obtained (A.1) and (A.2), combing them leads to

$$\begin{aligned}
c_1 \sigma_1 &\leq (c_1 + c_2 - 2\nu_2^{-1/3}t)\sigma_1 \\
&\leq \{c_1 + c_2 - (1 + \nu_2^{-1/3})t\}\sigma_1 + t\sigma_1\{1 + O_p(\nu_2^{-1/2})\} \\
&\leq c(0) - c(t, \nu_2) + t\widehat{\sigma}_1 \\
&\leq (c_1 + c_2)\sigma_1 + t\sigma_1\{1 + O_p(\nu_2^{-1/2})\} \\
&\leq 2(c_1 + c_2)\sigma_1,
\end{aligned}$$

where we used (A.1) and (A.2) to obtain the third and fourth inequalities above.

This implies the two rejection regions differ by a constant times σ_1 , i.e., $|c(0) - c(t, \nu_2) + t\widehat{\sigma}_1| \asymp \sigma_1$. □

D Proof of Theorem 2

Proof of result 1 from Theorem 2. For any $t \geq 0$, one can easily verify that there exists a positive constant u such that

$$\left| \frac{d}{dc} \omega\{c_0, \sigma_1, \nu_2, t, c\} \right| \leq u.$$

Therefore, by the mean value theorem, for any $t \geq 0$, there exists $\tilde{c}(t, \nu_2) \in (\widehat{c}(t, \nu_2), c(t, \nu_2))$ such that

$$\omega\{c_0, \sigma_1, \nu_2, t, \widehat{c}(t, \nu_2)\} = \alpha_0 + \frac{d}{dc}\omega\{c_0, \sigma_1, \nu_2, t, \tilde{c}(t, \nu_2)\}\{\widehat{c}(t, \nu_2) - c(t, \nu_2)\},$$

since $\omega\{c_0, \sigma_1, \nu_2, t, c(t, \nu_2)\} = \alpha_0$ as $\{t, c(t)\} \in \mathcal{A}(\alpha_0)$ in (6). Moreover, we have

$$\begin{aligned} |\omega\{c_0, \sigma_1, \nu_2, t, \widehat{c}(t, \nu_2)\} - \alpha_0| &= \frac{d}{dc}\omega\{c_0, \sigma_1, \nu_2, t, \tilde{c}(t, \nu_2)\}\{\widehat{c}(t, \nu_2) - c(t, \nu_2)\} \\ &\leq u |\widehat{c}(t, \nu_2) - c(t, \nu_2)| \\ &= O_p(\sigma_1/\sqrt{\nu_2}), \end{aligned}$$

where the last equality follows from Proposition 1. Therefore, we obtain

$$\omega\{c_0, \sigma_1, \nu_2, t, \widehat{c}(t, \nu_2)\} = \alpha_0 + O_p(\sigma_1/\sqrt{\nu_2}). \quad (\text{A.3})$$

□

Proof of result 2 from Theorem 2. Using $\omega\{\theta, \sigma_1, \nu_2, 0, \widehat{c}(0)\} = \omega\{\theta, \sigma_1, \nu_2, 0, c(0)\} + O_p(\sigma_1/\sqrt{\nu_2})$, and $\omega\{\theta, \sigma_1, \nu_2, t, \widehat{c}(t, \nu_2)\} = \omega\{\theta, \sigma_1, \nu_2, t, c(t, \nu_2)\} + O_p(\sigma_1/\sqrt{\nu_2})$, similarly to (A.3), we have $\omega\{\theta, \sigma_1, \nu_2, 0, \widehat{c}(0)\} - \omega\{\theta, \sigma_1, \nu_2, t, \widehat{c}(t, \nu_2)\} = \omega\{\theta, \sigma_1, \nu_2, 0, c(0)\} - \omega\{\theta, \sigma_1, \nu_2, t, c(t, \nu_2)\} + O_p(\sigma_1/\sqrt{\nu_2})$. As Theorem 1 ensures that $\omega\{\theta, \sigma_1, \nu_2, 0, c(0)\} - \omega\{\theta, \sigma_1, \nu_2, t, c(t, \nu_2)\} \geq 0$, it follows that, for sufficiently small σ_1/ν_2 , we have

$$\omega\{\theta, \sigma_1, \nu_2, 0, \widehat{c}(0)\} - \omega\{\theta, \sigma_1, \nu_2, t, \widehat{c}(t, \nu_2)\} \geq 0. \quad \square$$

E Computational details for univariate cTOST

Operationally, $\widehat{c}(0)$ can be efficiently computed through the following Newton–Raphson method. At iteration k , with $k \in \mathbb{N}$, we define

$$c^{(k+1)} = c^{(k)} + \widehat{\sigma}_1 \frac{\alpha_0 + \Phi\left(\frac{c_0 - c^{(k)}}{\widehat{\sigma}_1}\right) - \Phi\left(\frac{c_0 + c^{(k)}}{\widehat{\sigma}_1}\right)}{\varphi\left(\frac{c_0 + c^{(k)}}{\widehat{\sigma}_1}\right) + \varphi\left(\frac{c_0 - c^{(k)}}{\widehat{\sigma}_1}\right)}, \quad (\text{A.4})$$

where the procedure is initialized at

$$\begin{aligned} c^{(0)} &= I\{c_0 > \widehat{\sigma}_1 \Phi^{-1}(1 - \alpha_0)\} \{c_0 - \widehat{\sigma}_1 \Phi^{-1}(1 - \alpha_0)\} \\ &\quad + I\{c_0 \leq \widehat{\sigma}_1 \Phi^{-1}(1 - \alpha_0)\} c_0. \end{aligned} \quad (\text{A.5})$$

This choice for $c^{(0)}$ is motivated by the simple approximation $\alpha_0 = \Phi\left\{\frac{c_0 + \widehat{c}(0)}{\widehat{\sigma}_1}\right\} - \Phi\left\{\frac{c_0 - \widehat{c}(0)}{\widehat{\sigma}_1}\right\} \approx 1 - \Phi\left\{\frac{c_0 - \widehat{c}(0)}{\widehat{\sigma}_1}\right\}$ when $\widehat{\sigma}_1$ is sufficiently small. At convergence of the sequence $c^{(k)}$, we have $c^{(k)} = c^{(k+1)} = \widehat{c}(0)$. The procedure to compute the adjustment $\widehat{c}(0)$ is described in Algorithm 1.

Algorithm 1: Algorithm for computing the cTOST adjustment $\widehat{c}(0)$.

Input : nominal significance level α_0 , equivalence margins c_0 , standard error $\widehat{\sigma}_1$, degrees of freedom ν_2 , algorithmic tolerance ϵ_{\min} ;

Output: cTOST adjustment $\widehat{c}(0)$;

Initialize $c^{(0)}$ as in (A.5);

Obtain $c^{(1)}$ as in (A.4);

Set $k = 0$;

while $|c^{(k+1)} - c^{(k)}| > \epsilon_{\min}$ **do**

 | Set $k = k + 1$;

 | Obtain $c^{(k+1)}$ as in (A.4);

end

Output the cTOST adjustment $\widehat{c}(0) = c^{(k+1)}$;

Since the result of a bioequivalence assessment is often visualized through a confidence interval, cTOST allows this interpretation for sufficiently small $\widehat{\sigma}_1$. In this case, we have $c_0 > \widehat{c}(0)$ and we can consider the interval $\widehat{\theta} \pm \{c_0 - \widehat{c}(0)\}$, which allows us to use the IIP and accept H_1 if the interval falls entirely within the equivalence margins $(-c_0, c_0)$.

F A comparison of multivariate TOST adjustments

First, we illustrate in Figure A.2 how $\boldsymbol{\lambda}(\mathbf{t}, \mathbf{c})$ is affected by the structure of $\boldsymbol{\Sigma}_1$ when we set $\mathbf{t} = t_{\alpha_0, \nu_2} \mathbf{1}_K$, $\mathbf{c} = c_0 \mathbf{1}_K$ (i.e., for the conventional TOST procedure), and consider a simplified setting with $K = 2$, $\sigma_{1,1} = \sigma_{1,2} = 0.1$, $\nu_2 = 20$, $c_0 = \log(1.25)$, and $\alpha_0 = 0.05$.

To compare various methods, for simplicity, we consider a case where $K = 2$ and $\boldsymbol{\Sigma}_1$ is a diagonal matrix, with $c_0 = \log(1.25)$ and $\alpha_0 = 0.05$. We further focus on $\mathbf{t} = \mathbf{0}$

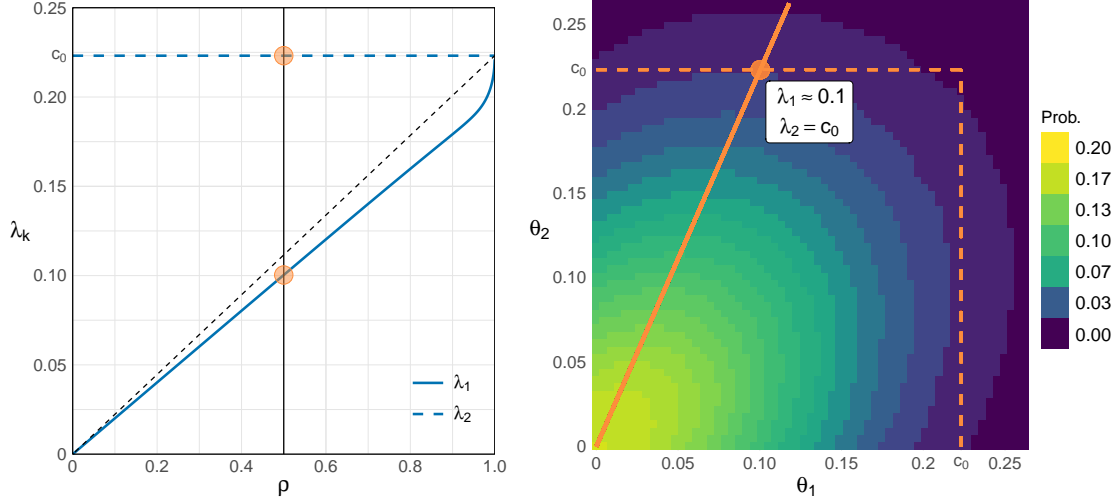


Figure A.2: Illustrative example of the complex relationship between $\boldsymbol{\lambda}$ in (11) and the covariance structure of $\widehat{\boldsymbol{\theta}}$ for the bivariate TOST, when $\sigma_{1,1} = \sigma_{1,2} = 0.1$, $\nu_2 = 20$, $c_0 = \log(1.25)$, and $\alpha_0 = 0.05$. Left panel: The λ_1 coordinate as a function of the correlation level $\rho \in [0, 1)$ between the components of $\widehat{\boldsymbol{\theta}}$, while λ_2 is fixed at c_0 . Orange dots indicate the coordinates of λ_k , for $k = 1, 2$, at $\rho = 0.5$. A black dashed line passing through the origin with slope c_0 serves as a benchmark. Right panel: Probability that bivariate TOST rejects H_0 at $\boldsymbol{\theta} = (\theta_1, \theta_2)^\top$ in the upper right quadrant when $\rho = 0.5$. The orange dashed lines mark the boundary separating the H_0 and H_1 regions. The orange dot represents a choice of $\boldsymbol{\lambda}$ (corresponding to $\lambda_2 = c_0$, as in the left panel). The orange solid line, connecting the origin to $\boldsymbol{\lambda}$, illustrates the method-specific trajectory of $\boldsymbol{\theta}$ used for comparing different methods in the numerical study of Section 4.2.

and restrict ourselves to adjustments $\{\mathbf{0}, \mathbf{c}(\mathbf{0})\} \in \mathcal{A}_K^*(\alpha_0)$. In this simplified setting, it can be shown that $\boldsymbol{\lambda}$ in (11) corresponds either to $\boldsymbol{\lambda}_1 \equiv (c_0, 0)^\top$ or $\boldsymbol{\lambda}_2 \equiv (0, c_0)^\top$, in the sense that $\boldsymbol{\lambda} = \operatorname{argmax}_{\boldsymbol{\tau} \in \{\boldsymbol{\lambda}_1, \boldsymbol{\lambda}_2\}} \omega_K\{\boldsymbol{\tau}, \boldsymbol{\Sigma}_1, \nu_2, \mathbf{0}, \mathbf{c}(\mathbf{0})\}$. Moreover, for a fixed value of c_2 , when a solution to the matching in (10) exists, there is a unique adjustment $c_1(0)$ leading to a size of α_0 . We thus consider a family of adjustments $\mathbf{c}(\mathbf{0}) =$

$\{c_1(0), c_2\}^T$. Figure A.3 illustrates how varying c_2 affects $c_1(0)$ (first row), the power at $\boldsymbol{\theta} = (0, 0)^T$ (second row), as well as the marginal sizes (third row). The columns of Figure A.3 represent different configurations of $\sigma_{1,2} \in \{0.1, 0.12, 0.14\}$ while keeping $\sigma_{1,1}$ fixed at 0.1. Within each panel, the regions shaded in lighter and darker grays denote the areas where $\boldsymbol{\lambda}$ corresponds to $\boldsymbol{\lambda}_1$ and $\boldsymbol{\lambda}_2$, respectively. The proposed multivariate cTOST corresponds to the adjustment that leads to equal marginal sizes, that is, $(\mathbf{0}, \mathbf{c}^*) \in \mathcal{A}_K(\alpha_0)$ in (12) where \mathbf{c}^* is defined in (13)-(15), and its operating characteristics are highlighted with orange dots in the panels of Figure A.3. We contrast \mathbf{c}^* with another very natural adjustment, say $\{\mathbf{0}, \tilde{\mathbf{c}}(\mathbf{0})\} \in \mathcal{A}_K^*(\alpha_0)$ in (10), corresponding to the one that maximizes the power at $(0, 0)$, whose operating characteristics are highlighted with blue circles in the panels of Figure A.3. Although the two solutions \mathbf{c}^* and $\tilde{\mathbf{c}}(\mathbf{0})$ coincide under homoskedasticity, they get further apart in the presence of stronger forms of heteroskedasticity (first row). More specifically, in the latter case, \mathbf{c}^* sacrifices a bit of power (second row) but maintains a balanced marginal risk across all dimensions (third row), in the sense that the type I error rate is evenly split across its components. On the other hand, $\tilde{\mathbf{c}}(\mathbf{0})$ may lead to very unbalanced marginal sizes, whose difference is close to 20% on the third column of Figure A.3. Thus, the rejection regions associated with $\tilde{\mathbf{c}}(\mathbf{0})$ may be quite uneven across its components. This is further illustrated in Figure A.4, where we compare the rejection regions of bivariate TOST, cTOST, and the “other” potential adjustment

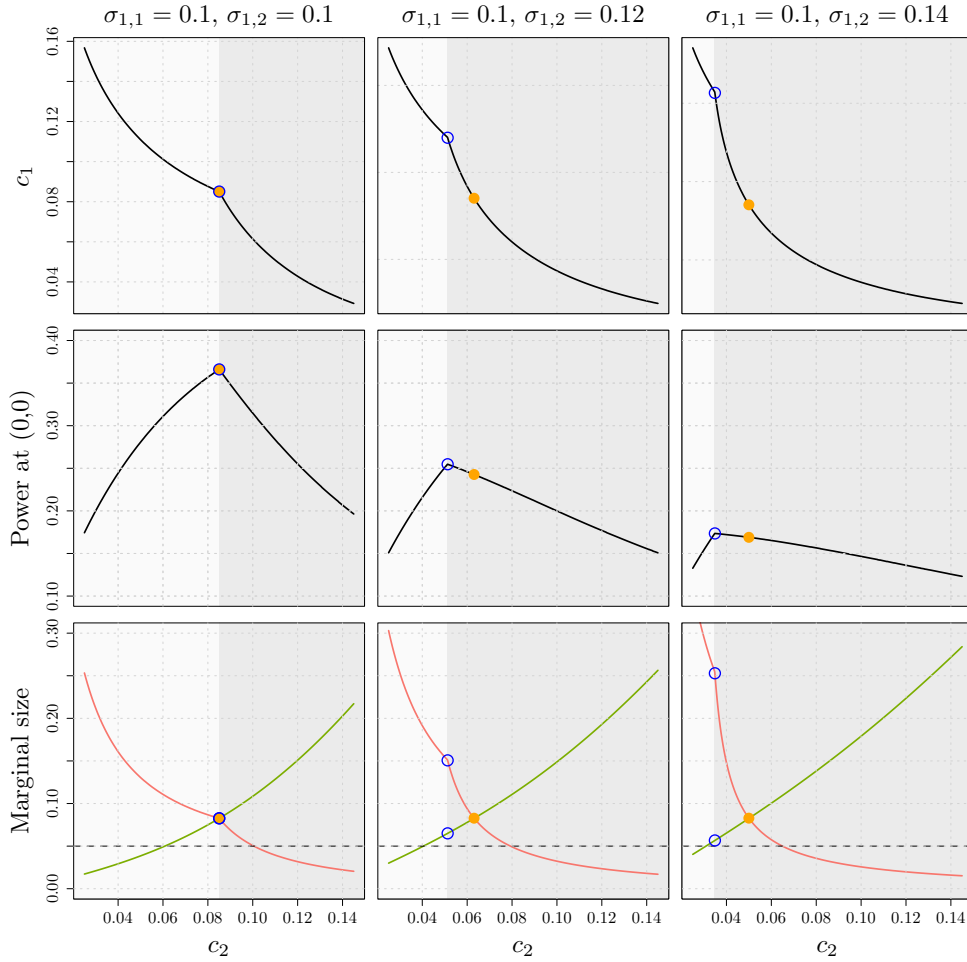


Figure A.3: Adjustment $c_1(0)$ when considering $\mathbf{c}(\mathbf{0}) = \{c_1(0), c_2\}^T$ such that $\{\mathbf{0}, \mathbf{c}(\mathbf{0})\} \in \mathcal{A}_K^*(\alpha_0)$ (first row), corresponding power at $\boldsymbol{\theta} = (0, 0)^T$ (second row), and marginal sizes, respectively highlighted in red and green across the two components, where the dashed horizontal line is at the nominal $\alpha_0 = 5\%$ (third row), across various configurations of $\sigma_{1,2} \in \{0.1, 0.12, 0.14\}$ (from left to right columns) when $\sigma_{1,1} = 0.1$. The multivariate cTOST, $(\mathbf{0}, \mathbf{c}^*) \in \mathcal{A}_K(\alpha_0)$, leads to equal marginal sizes, and its operating characteristics are highlighted with orange dots. The “other” adjustment $\{\mathbf{0}, \tilde{\mathbf{c}}(\mathbf{0})\} \in \mathcal{A}_K^*(\alpha_0)$ maximizes the power at $\boldsymbol{\theta} = (0, 0)^T$, and its operating characteristics are highlighted with blue circles. Regions shaded in lighter and darker grays denote the areas where $\boldsymbol{\lambda}$ corresponds to $\boldsymbol{\lambda}_1$ and $\boldsymbol{\lambda}_2$, respectively.

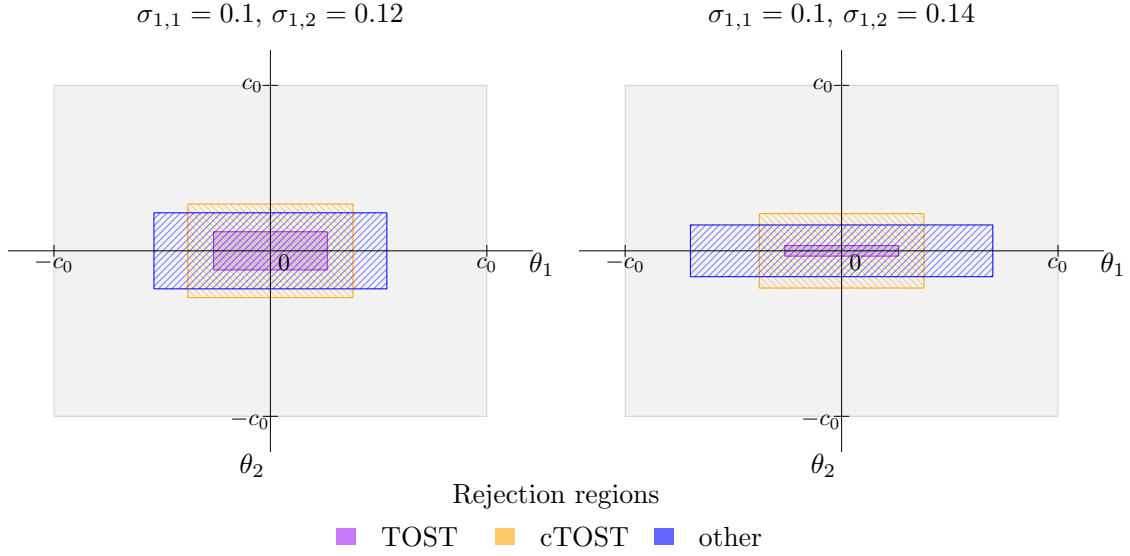


Figure A.4: Comparison of the rejection regions of bivariate TOST, cTOST, and the “other” potential adjustment based on $\{\mathbf{0}, \tilde{\mathbf{c}}(\mathbf{0})\} \in \mathcal{A}_K^*(\alpha_0)$, when $\sigma_{1,2} = 0.12$ (left), $\sigma_{1,2} = 0.14$ (right) and $\sigma_{1,1} = 0.1$.

based on $\tilde{\mathbf{c}}(\mathbf{0})$. The two panels correspond to the covariance structures respectively used for the second and third column of Figure A.3.

G Equivalence of all adjustments in $\mathcal{A}_K(\alpha_0)$ when Σ_1 is known

In this section, we assume that Σ_1 is known, so that the (multivariate) canonical form defined in (2) only relies on the distribution of $\hat{\boldsymbol{\theta}}$, which is Gaussian. Similarly to Appendix A, we consider a more flexible counterpart of the multivariate TOST that relies on z -statistics rather than t -statistics. Namely, consider (\mathbf{z}, \mathbf{c}) such that

the multivariate rejection region of this test is

$$C_K(\mathbf{z}, \mathbf{c}) = \left\{ \widehat{\boldsymbol{\theta}} \in \mathbb{R}^K : \bigcap_{k=1}^K \left(z_k \sigma_{1,k} - c_k < \widehat{\theta}_k < c_k - z_k \sigma_{1,k} \right) \right\}, \quad (\text{A.6})$$

where $\mathbf{z} \equiv (z_1, \dots, z_K)^\text{T}$ and $\mathbf{c} \equiv (c_1, \dots, c_K)^\text{T}$. The corresponding probability of rejecting H_0 is expressed as

$$\begin{aligned} \omega_K\{\boldsymbol{\theta}, \boldsymbol{\Sigma}_1, \infty, \mathbf{z}, \mathbf{c}\} &= \Pr\{\widehat{\boldsymbol{\theta}} \in C_K(\mathbf{z}, \mathbf{c})\} \\ &= \Pr \left\{ \bigcap_{k=1}^K \left(z_k - \frac{c_k}{\sigma_{1,k}} - \frac{\theta_k}{\sigma_{1,k}} < \frac{\widehat{\theta}_k - \theta_k}{\sigma_{1,k}} < \frac{c_k}{\sigma_{1,k}} - z_k - \frac{\theta_k}{\sigma_{1,k}} \right) \right\}. \end{aligned} \quad (\text{A.7})$$

Then, as a counterpart of (12), we restrict ourselves to corrective procedures belonging to the set $\mathcal{A}_K(\alpha_0)$, such that

$$\begin{aligned} \mathcal{A}_K(\alpha_0) &= \{(\mathbf{z}, \mathbf{c}) : \mathbf{z} \in \mathbb{R}_{\geq 0}^K, \mathbf{c} \in \mathbb{R}_{> 0}^K, \omega_K\{\boldsymbol{\lambda}(\boldsymbol{\Sigma}_1, \mathbf{z}, \mathbf{c}), \boldsymbol{\Sigma}_1, \infty, \mathbf{z}, \mathbf{c}\} = \alpha_0, \\ &\quad \omega(c_0, \sigma_{1,1}, \infty, z_1, c_1) = \dots = \omega(c_0, \sigma_{1,K}, \infty, z_K, c_K)\}, \end{aligned} \quad (\text{A.8})$$

and

$$\boldsymbol{\lambda}(\boldsymbol{\Sigma}_1, \mathbf{z}, \mathbf{c}) = (\lambda_1, \dots, \lambda_K)^\text{T} \in \boldsymbol{\Lambda}(\boldsymbol{\Sigma}_1, \mathbf{z}, \mathbf{c}) \equiv \underset{\boldsymbol{\theta} \notin (-c_0, c_0)^K}{\text{argsup}} \omega_K\{\boldsymbol{\theta}, \boldsymbol{\Sigma}_1, \infty, \mathbf{z}, \mathbf{c}\}.$$

As in the univariate setting described in Appendix A, we next show that (A.8) provides a unique $\mathbf{c}(\mathbf{z})$ for any subjectively selected $\mathbf{z} \in \mathbb{R}_{\geq 0}^K$. Specifically, first,

note that $c_k(\mathbf{z})$, such that $\{z_k, c_k(\mathbf{z})\} \in \mathcal{A}(\gamma)$, for $k = 1, \dots, K$, is strictly increasing with respect to γ (see the discussion following (6)), and hence the corresponding probability of rejecting H_0 , $\omega_K\{\boldsymbol{\theta}, \boldsymbol{\Sigma}_1, \nu_2, \mathbf{z}, \mathbf{c}(\mathbf{z})\}$, is also strictly increasing with γ at any $\boldsymbol{\theta} \in \mathbb{R}^K$. Therefore, there exists a unique γ^* (see (A.9) below) such that $\omega_K\{\boldsymbol{\lambda}(\boldsymbol{\Sigma}_1, \mathbf{z}, \mathbf{c}), \boldsymbol{\Sigma}_1, \infty, \mathbf{z}, \mathbf{c}(\mathbf{z})\} = \alpha_0$ in (A.8). Next, constraining the marginal sizes to

$$\omega\{c_0, \sigma_{1,1}, \infty, z_1, c_1(\mathbf{z})\} = \dots = \omega\{c_0, \sigma_{1,K}, \infty, z_K, c_K(\mathbf{z})\} = \gamma^* \quad (\text{A.9})$$

yields a unique rejection region in (A.6) for any choice of \mathbf{z} , due to the argument presented in Appendix A for the univariate setting. Thus, it follows that all corrective procedures $\{\mathbf{z}, \mathbf{c}(\mathbf{z})\} \in \mathcal{A}_K(\alpha_0)$ provide the same rejection region in (A.6) regardless of the choice of \mathbf{z} . Therefore, these procedures are equivalent in terms of their probability of rejecting H_0 , in the sense that $\omega_K\{\boldsymbol{\theta}, \boldsymbol{\Sigma}_1, \infty, \mathbf{z}, \mathbf{c}(\mathbf{z})\}$, at any $\boldsymbol{\theta} \in \mathbb{R}^K$, does not change as \mathbf{z} changes.

Finally, the multivariate cTOST in (13)-(15) is equivalent to the corrective procedures $\{\mathbf{z}, \mathbf{c}(\mathbf{z})\} \in \mathcal{A}_K(\alpha_0)$ in (A.8). This arises from the fact that its probability of rejecting H_0 , which is $\omega_K(\boldsymbol{\theta}, \boldsymbol{\Sigma}_1, \nu_2, \mathbf{0}, \mathbf{c}^*)$ defined in (9), takes the same form of $\omega_K\{\boldsymbol{\theta}, \boldsymbol{\Sigma}_1, \infty, \mathbf{z}, \mathbf{c}(\mathbf{z})\}$ in (A.7) and, based on the result provided in Appendix A, the marginal rejection regions implied by $(0, c_k^*)$ in (15) and $\{z_k, c_k(\mathbf{z})\}$ in (A.9) are the same for every $k = 1, \dots, K$. Therefore, it follows that $\omega_K(\boldsymbol{\theta}, \boldsymbol{\Sigma}_1, \nu_2, \mathbf{0}, \mathbf{c}^*) =$

$\omega_K\{\boldsymbol{\theta}, \boldsymbol{\Sigma}_1, \infty, \mathbf{0}, \mathbf{c}(\mathbf{0})\} = \omega_K\{\boldsymbol{\theta}, \boldsymbol{\Sigma}_1, \infty, \mathbf{z}, \mathbf{c}(\mathbf{z})\}$ for any $\boldsymbol{\theta} \in \mathbb{R}^K$.

H Properties of the multivariate cTOST under independence

In this section, we restrict our attention to adjustments $(\mathbf{t}, \mathbf{c}) \in \mathcal{A}_K(\alpha_0)$ in (12). We first introduce the following lemma to characterize the set of parameter values $\boldsymbol{\Lambda}$ in (11) at which we evaluate the test size under independence. In this case, under both homoskedasticity and heteroskedasticity, the size is always evaluated at one of the intersections with the coordinate axes.

Lemma 1. Assume that $\boldsymbol{\Sigma}_1 = \text{diag}(\sigma_{1,1}^2, \dots, \sigma_{1,K}^2)$ where $\text{diag}(\cdot)$ denotes a diagonal matrix, and consider $\{\mathbf{t}, \mathbf{c}(\mathbf{t})\} \in \mathcal{A}_K(\alpha_0)$ in (12). It follows that $\boldsymbol{\Lambda}$ in (11) satisfies

$$\boldsymbol{\Lambda}\{\boldsymbol{\Sigma}_1, \nu_2, \mathbf{t}, \mathbf{c}(\mathbf{t})\} \subseteq \{c_0\mathbf{e}_1, \dots, c_0\mathbf{e}_K, -c_0\mathbf{e}_1, \dots, -c_0\mathbf{e}_K\},$$

where \mathbf{e}_h is the h th standard basis vector in \mathbb{R}^K .

Proof of Lemma 1. We recall that $\{\mathbf{t}, \mathbf{c}(\mathbf{t})\} \in \mathcal{A}_K(\alpha_0)$ in (12) leads to

$$\omega_K\{\boldsymbol{\lambda}, \boldsymbol{\Sigma}_1, \nu_2, \mathbf{t}, \mathbf{c}(\mathbf{t})\} = \prod_{k=1}^K \omega\{\lambda_k, \sigma_{1,k}, \nu_2, t_k, c_k(\mathbf{t})\} = \alpha_0, \quad (\text{A.10})$$

and equal marginal sizes

$$\omega\{c_0, \sigma_{1,1}, \nu_2, t_1, c_1(\mathbf{t})\} = \dots = \omega\{c_0, \sigma_{1,K}, \nu_2, t_K, c_K(\mathbf{t})\}, \quad (\text{A.11})$$

where the first equality in (A.10) holds due to independence. Let h satisfy

$$\omega\{0, \sigma_{1,h}, \nu_2, t_h, c_h(\mathbf{t})\} \leq \omega\{0, \sigma_{1,u}, \nu_2, t_u, c_u(\mathbf{t})\} \quad (\text{A.12})$$

for all $u \in \{1, \dots, K\}$, i.e., h corresponds to the smallest marginal power at $\theta = 0$.

Note that $\omega\{\theta, \sigma_{1,k}, \nu_2, t_k, c_k(\mathbf{t})\}$ is non-increasing in $\theta \in \mathbb{R}_{\geq 0}$, for any $k = 1, \dots, K$,

and that to satisfy (11) at least one component of $\boldsymbol{\lambda} \equiv \boldsymbol{\lambda}(\mathbf{t}, \mathbf{c}) \in \boldsymbol{\Lambda}\{\boldsymbol{\Sigma}_1, \nu_2, \mathbf{t}, \mathbf{c}(\mathbf{t})\}$

in (11) has to be on the boundary $\pm c_0$. Therefore, since all K components have the

same marginal size due to (A.11), based on (A.10) and (A.12) we get

$$\sup_{\boldsymbol{\theta} \notin (-c_0, c_0)^K} \omega_K(\boldsymbol{\theta}, \boldsymbol{\Sigma}_1, \nu_2, \mathbf{t}, \mathbf{c}) = \omega\{c_0, \sigma_{1,h}, \nu_2, t_h, c_h(\mathbf{t})\} \prod_{\substack{k \in \{1, \dots, K\}, \\ k \neq h}} \omega\{0, \sigma_{1,k}, \nu_2, t_k, c_k(\mathbf{t})\}.$$

This implies that the set $\boldsymbol{\Lambda}\{\boldsymbol{\Sigma}_1, \nu_2, \mathbf{t}, \mathbf{c}(\mathbf{t})\}$ only contains vectors of the form $\boldsymbol{\lambda}_h \equiv$

$c_0 \mathbf{e}_h$, where the h th component satisfies (A.12), thus completing the proof. \square

As a direct consequence of Lemma 1, the following corollary provides, as a special case, the set $\boldsymbol{\Lambda}$ in (14) at which we evaluate the test size of multivariate cTOST under homoskedasticity.

Corollary 1: Assume that $\Sigma_1 = \sigma_1^2 \mathbf{I}_K$, and consider $\{\mathbf{t}, \mathbf{c}(\mathbf{t})\} \in \mathcal{A}_K(\alpha_0)$ in (12) such that $\mathbf{t} = t\mathbf{1}_K$ with $t \geq 0$. Then, Λ in (11) satisfies

$$\Lambda\{\Sigma_1, \nu_2, \mathbf{t}, \mathbf{c}(\mathbf{t})\} = \{c_0 \mathbf{e}_1, \dots, c_0 \mathbf{e}_K, -c_0 \mathbf{e}_1, \dots, -c_0 \mathbf{e}_K\}.$$

Proof of Corollary 1. The result follows immediately from Lemma 1 since all K components in (A.12) have same marginal power, in the sense that

$$\omega\{\theta, \sigma_1, \nu_2, t_1, c_1(\mathbf{t})\} = \dots = \omega\{\theta, \sigma_1, \nu_2, t_K, c_K(\mathbf{t})\},$$

for any $\theta \in \mathbb{R}$. □

In the rest of this section, we restrict our attention to the independent and homoskedastic setting, where $\Sigma_1 = \sigma_1^2 \mathbf{I}_K$. To assess the statistical power in declaring bioequivalence for adjustments $\{\mathbf{t}, \mathbf{c}(\mathbf{t})\} \in \mathcal{A}_K(\alpha_0)$, that is, $\omega_K\{\boldsymbol{\theta}, \Sigma_1, \nu_2, \mathbf{t}, \mathbf{c}(\mathbf{t})\}$ defined in (9) for some $\boldsymbol{\theta} \in (-c_0, c_0)^K$, we begin by establishing Lemma 2, which will be used in the proofs for Proposition 2 and Proposition 3 presented below, where we respectively consider $\boldsymbol{\theta} = \mathbf{0}$ and $\boldsymbol{\theta}$ in a neighborhood of $c_0 \mathbf{1}_K$.

Lemma 2. Assume that $\Sigma_1 = \sigma_1^2 \mathbf{I}_K$, and consider the adjustments $\{\mathbf{t}, \mathbf{c}(\mathbf{t})\}$ and $\{\mathbf{0}, \mathbf{c}(\mathbf{0})\}$ belonging to $\mathcal{A}_K(\alpha_0)$ in (12). The (global) size- α_0 constraint in (12) re-

spectively leads to

$$\omega_K\{\boldsymbol{\lambda}_h, \boldsymbol{\Sigma}_1, \nu_2, \mathbf{t}, \mathbf{c}(\mathbf{t})\} = \omega\{c_0, \sigma_1, \nu_2, t_h, c_h(\mathbf{t})\} \prod_{\substack{k \in \{1, \dots, K\}, \\ k \neq h}} \omega\{0, \sigma_1, \nu_2, t_k, c_k(\mathbf{t})\} = \alpha_0, \quad (\text{A.13})$$

$$\omega_K\{\boldsymbol{\lambda}_g, \boldsymbol{\Sigma}_1, \nu_2, \mathbf{0}, \mathbf{c}(\mathbf{0})\} = \omega\{c_0, \sigma_1, \nu_2, 0, c_g(\mathbf{0})\} \prod_{\substack{k \in \{1, \dots, K\}, \\ k \neq g}} \omega\{0, \sigma_1, \nu_2, 0, c_k(\mathbf{0})\} = \alpha_0, \quad (\text{A.14})$$

where $\boldsymbol{\lambda}_k$ (for $k = 1, \dots, K$) is defined in the proof of Lemma 1, $h \in \{1, \dots, K\}$, and $g = 1, \dots, K$, subject to marginal size constraints

$$\{t_k, c_k(\mathbf{t})\} \in \mathcal{A}\{\gamma(\mathbf{t})\}, \quad (\text{A.15})$$

$$\{0, c_k(\mathbf{0})\} \in \mathcal{A}(\gamma), \quad (\text{A.16})$$

for $k = 1, \dots, K$, where $\mathcal{A}(\cdot)$ is defined in (6) and $\gamma \equiv \gamma(\mathbf{0}) \leq \gamma(\mathbf{t})$.

Proof of Lemma 2. The first equality in (A.13) follows immediately from Lemma 1, which ensures the existence of at least one such $h \in \{1, \dots, K\}$ at any \mathbf{t} . The second equality of (A.13) follows from the fact that $\{\mathbf{t}, \mathbf{c}(\mathbf{t})\}$ leads to the global size α_0 as it belongs to $\mathcal{A}_K(\alpha_0)$ in (12). Considering the special case of $\mathbf{t} = \mathbf{0}$ leads to (A.14).

We next show that $\gamma \leq \gamma(\mathbf{t})$ by contradiction. Assume $\gamma > \gamma(\mathbf{t})$. Note that $\omega\{c_0, \sigma_1, \nu_2, t_h, c_h(\mathbf{t})\} = \gamma(\mathbf{t})$ and $\omega\{c_0, \sigma_1, \nu_2, 0, c_g(\mathbf{0})\} = \gamma$. For any $k \neq h$, let

$\tilde{c}_k(s)$ be the function of s such that $\omega\{c_0, \sigma_1, \nu_2, s, \tilde{c}_k(s)\} = \gamma(\mathbf{t})$ for all s . Because $\omega\{c_0, \sigma_1, \nu_2, 0, \tilde{c}_k(0)\}$ is an increasing function of $\tilde{c}_k(0)$ (see the discussion following (6)), from

$$\gamma = \omega\{c_0, \sigma_1, \nu_2, 0, c_k(\mathbf{0})\} > \omega\{c_0, \sigma_1, \nu_2, 0, \tilde{c}_k(0)\} = \gamma(\mathbf{t}) = \omega\{c_0, \sigma_1, \nu_2, t_k, c_k(\mathbf{t})\},$$

we obtain $c_k(\mathbf{0}) > \tilde{c}_k(0)$. Then

$$\omega\{0, \sigma_1, \nu_2, 0, c_k(\mathbf{0})\} > \omega\{0, \sigma_1, \nu_2, 0, \tilde{c}_k(0)\} \geq \omega\{0, \sigma_1, \nu_2, t_k, c_k(\mathbf{t})\},$$

where the first inequality is because of $c_k(\mathbf{0}) > \tilde{c}_k(0)$ and $\omega\{0, \sigma_1, \nu_2, 0, c_k(\mathbf{0})\}$ is an increasing function of $c_k(\mathbf{0})$, the second inequality is due to Theorem 1. Thus, (A.14) leads to

$$\begin{aligned} \alpha_0 &= \gamma \prod_{\substack{k \in \{1, \dots, K\}, \\ k \neq g}} \omega\{0, \sigma_1, \nu_2, 0, c_k(\mathbf{0})\} \\ &= \frac{\gamma \omega\{0, \sigma_1, \nu_2, 0, c_h(\mathbf{0})\}}{\omega\{0, \sigma_1, \nu_2, 0, c_g(\mathbf{0})\}} \prod_{\substack{k \in \{1, \dots, K\}, \\ k \neq h}} \omega\{0, \sigma_1, \nu_2, 0, c_k(\mathbf{0})\} \\ &= \gamma \prod_{\substack{k \in \{1, \dots, K\}, \\ k \neq h}} \omega\{0, \sigma_1, \nu_2, 0, c_k(\mathbf{0})\} \\ &> \gamma \prod_{\substack{k \in \{1, \dots, K\}, \\ k \neq h}} \omega\{0, \sigma_1, \nu_2, t_k, c_k(\mathbf{t})\} \\ &= \gamma / \gamma(\mathbf{t}) \alpha_0, \end{aligned}$$

which leads to $\gamma(\mathbf{t}) > \gamma$, contradicting our assumption. Hence $\gamma \leq \gamma(\mathbf{t})$. \square

We next present the proof of Proposition 2 in Section 3.2. Here, under homoskedasticity and independence, we aim to show that the probability of declaring bioequivalence at $\boldsymbol{\theta} = \mathbf{0}$, within the class of adjustments $\{\mathbf{t}, \mathbf{c}(\mathbf{t})\} \in \mathcal{A}_K(\alpha_0)$ in (12), is maximized by multivariate cTOST.

Proof of Proposition 2. For $\{\mathbf{t}, \mathbf{c}(\mathbf{t})\} \in \mathcal{A}_K(\alpha_0)$, it follows that

$$\begin{aligned} \omega\{0, \sigma_1, \nu_2, t_h, c_h(\mathbf{t})\} &\leq \min_{\substack{k \in \{1, \dots, K\}, \\ k \neq h}} [\omega\{0, \sigma_1, \nu_2, t_k, c_k(\mathbf{t})\}] \\ &\leq \left(\prod_{\substack{k \in \{1, \dots, K\}, \\ k \neq h}} [\omega\{0, \sigma_1, \nu_2, t_k, c_k(\mathbf{t})\}] \right)^{1/(K-1)} \\ &= \left(\frac{\alpha_0}{\gamma(\mathbf{t})} \right)^{\frac{1}{K-1}}, \end{aligned} \tag{A.17}$$

where the first inequality uses (A.12), and the last equality uses (A.13) and (A.15).

Similarly, due to Corollary 1, for any $k = 1, \dots, K$,

$$\omega\{0, \sigma_1, \nu_2, 0, c_k(\mathbf{0})\} = \left(\frac{\alpha_0}{\gamma} \right)^{\frac{1}{K-1}}, \tag{A.18}$$

based on (A.14) and (A.16). We thus obtain

$$\begin{aligned}
\omega_K\{\mathbf{0}, \boldsymbol{\Sigma}_1, \nu_2, \mathbf{t}, \mathbf{c}(\mathbf{t})\} &= \prod_{k=1}^K \omega\{0, \sigma_1, \nu_2, t_k, c_k(\mathbf{t})\} \\
&\leq \left(\frac{\alpha_0}{\gamma(\mathbf{t})}\right)^{\frac{1}{K-1}} \frac{\alpha_0}{\gamma(\mathbf{t})} \\
&\leq \left(\frac{\alpha_0}{\gamma}\right)^{\frac{K}{K-1}} \\
&= \prod_{k=1}^K \omega\{0, \sigma_1, \nu_2, 0, c_k(\mathbf{0})\} \\
&= \omega_K\{\mathbf{0}, \boldsymbol{\Sigma}_1, \nu_2, \mathbf{0}, \mathbf{c}(\mathbf{0})\}.
\end{aligned}$$

□

Despite the optimality of multivariate cTOST at $\boldsymbol{\theta} = \mathbf{0}$, shown in Proposition 2, Proposition 3 illustrates that a uniformly most powerful test for any $\boldsymbol{\theta} \in (-c_0, c_0)^K$ is generally not achievable in multivariate settings, even if we only consider the independence and homoskedasticity setting. This is very different from the univariate case.

Proposition 3: *At any given ν_2, σ_1 , consider $\boldsymbol{\Sigma}_1 = \sigma_1^2 \mathbf{I}_K$. The family of adjustments $(\mathbf{t}, \mathbf{c}) \in \mathcal{A}_K(\alpha_0)$ defined in (12) does not contain an optimal member $(\mathbf{t}_u, \mathbf{c}_u)$ that satisfies*

$$\omega_K\{\boldsymbol{\theta}, \boldsymbol{\Sigma}_1, \nu_2, \mathbf{t}, \mathbf{c}\} \leq \omega_K\{\boldsymbol{\theta}, \boldsymbol{\Sigma}_1, \nu_2, \mathbf{t}_u, \mathbf{c}_u\},$$

for any $\boldsymbol{\theta} \in (-c_0, c_0)^K$. Therefore, under independence and homoskedasticity, among all (globally) level- α_0 tests with equal marginal sizes, a uniformly most powerful test for the hypotheses in (1) does not exist.

Proof of Proposition 3. We prove this result by contradiction. Assume there exists an optimal \mathbf{t}_u so that $\{\mathbf{t}_u, \mathbf{c}_u(\mathbf{t}_u)\} \in \mathcal{A}_K(\alpha_0)$ satisfies

$$h(\boldsymbol{\theta}, \sigma_1^2 \mathbf{I}_K, \mathbf{t}_u, \mathbf{t}) \equiv \omega_K\{\boldsymbol{\theta}, \sigma_1^2 \mathbf{I}_K, \nu_2, \mathbf{t}_u, \mathbf{c}_u(\mathbf{t}_u)\} - \omega_K\{\boldsymbol{\theta}, \sigma_1^2 \mathbf{I}_K, \nu_2, \mathbf{t}, \mathbf{c}(\mathbf{t})\} \geq 0, \quad (\text{A.19})$$

for all $\{\mathbf{t}, \mathbf{c}(\mathbf{t})\} \in \mathcal{A}_K(\alpha_0)$ and any $\boldsymbol{\theta} \in (-c_0, c_0)^K$, σ_1 , and ν_2 . Hence, Proposition 2 and Lemma 2 lead to $\gamma(\mathbf{t}_u) = \gamma$. However, since not all tests achieve the optimal power at $\boldsymbol{\theta} = \mathbf{0}$ for all σ_1 , it is possible to find an instance of \mathbf{t} and σ_1 , say \mathbf{t}_l and σ_l , so that $\{\mathbf{t}_l, \mathbf{c}(\mathbf{t}_l)\} \in \mathcal{A}_K(\alpha_0)$, and $h(\mathbf{0}, \sigma_l^2 \mathbf{I}_K, \mathbf{t}_u, \mathbf{t}_l) > 0$. Moreover, let $t_{l,h}$ satisfy

$$\omega\{0, \sigma_l, \nu_2, t_{l,h}, c_h(\mathbf{t}_l)\} \leq \omega\{0, \sigma_l, \nu_2, t_{l,k}, c_k(\mathbf{t}_l)\},$$

for all $k = 1, \dots, K$, where $\{t_{l,k}, c_k(\mathbf{t}_l)\} \in \mathcal{A}\{\gamma(\mathbf{t}_l)\}$ and $\gamma(\mathbf{t}_l) \geq \gamma$ by Lemma 2. Hence, to satisfy $h(\mathbf{0}, \sigma_l^2 \mathbf{I}_K, \mathbf{t}_u, \mathbf{t}_l) > 0$, it follows that

$$\omega\{0, \sigma_l, \nu_2, t_{u,k}, c_k(\mathbf{t}_u)\} = \left[\frac{\alpha_0}{\gamma} \right]^{\frac{1}{K-1}} > \omega\{0, \sigma_l, \nu_2, t_{l,h}, c_h(\mathbf{t}_l)\},$$

where the equality is due to Proposition 2. Then, note that $\omega\{0, \sigma_l, \nu_2, t_{l,h}, c_h(\mathbf{t}_l)\}$

is an increasing function of $c_h(\mathbf{t}_l)$ (see the discussion following (6)), and consider $\mathbf{t}_l^* \equiv t_{l,h} \mathbf{1}_K$ such that $\{\mathbf{t}_l^*, \mathbf{c}(\mathbf{t}_l^*)\} \in \mathcal{A}_K(\alpha_0)$. This leads to $\{t_{l,k}^*, c_k(\mathbf{t}_l^*)\} \in \mathcal{A}\{\gamma(\mathbf{t}_l^*)\}$, for all $k = 1, \dots, K$, with $\gamma(\mathbf{t}_l^*) > \gamma$. Therefore, we obtain

$$h(\mathbf{0}, \sigma_l^2 \mathbf{I}_K, \mathbf{t}_u, \mathbf{t}_l^*) = \left[\frac{\alpha_0}{\gamma} \right]^{\frac{K}{K-1}} - \left[\frac{\alpha_0}{\gamma(\mathbf{t}_l^*)} \right]^{\frac{K}{K-1}} > 0.$$

Now, we have $h(c_0 \mathbf{1}_K, \sigma_l^2 \mathbf{I}_K, \mathbf{t}_u, \mathbf{t}_l^*) = \gamma^K - \gamma(\mathbf{t}_l^*)^K < 0$. Hence at a point $(c_0 - \epsilon) \mathbf{1}_K$, where $\epsilon > 0$ is a small value, which is very close to $c_0 \mathbf{1}_K$, we also have $h\{(c_0 - \epsilon) \mathbf{1}_K, \sigma_l^2 \mathbf{I}_K, \mathbf{t}_u, \mathbf{t}_l^*\} = \gamma^K - \gamma(\mathbf{t}_l^*)^K < 0$ due to continuity, which is contradictory to the optimality of \mathbf{t}_u at any $\boldsymbol{\theta} \in (-c_0, c_0)^K$ and any σ_1 . \square

As a direct consequence of Proposition 3, the following corollary ensures that a uniformly most powerful test for any $\boldsymbol{\theta} \in (-c_0, c_0)^K$ is generally not achievable in multivariate settings.

Corollary 2: *The family of adjustments $(\mathbf{t}, \mathbf{c}) \in \mathcal{A}_K(\alpha_0)$ defined in (12) does not contain an optimal member $(\mathbf{t}_u, \mathbf{c}_u)$ that satisfies*

$$\omega_K\{\boldsymbol{\theta}, \boldsymbol{\Sigma}_1, \nu_2, \mathbf{t}, \mathbf{c}\} \leq \omega_K\{\boldsymbol{\theta}, \boldsymbol{\Sigma}_1, \nu_2, \mathbf{t}_u, \mathbf{c}_u\},$$

for any $\boldsymbol{\theta} \in (-c_0, c_0)^K$ at any $\nu_2, \boldsymbol{\Sigma}_1$. Therefore, among all (globally) level- α_0 tests with equal marginal sizes, a uniformly most powerful test for the hypotheses in (1)

does not exist.

Proof of Corollary 2. The result follows immediately from Proposition 3. \square

Although Corollary 2 shows that a uniformly most powerful test does not exist in $\mathcal{A}_K(\alpha_0)$, we conjecture that the optimality of the multivariate cTOST at $\boldsymbol{\theta} = \mathbf{0}$ holds in situations more general than $\sigma_1^2 \mathbf{I}_K$, as required in Proposition 2. This conjecture is supported by extensive numerical results, and in Figure A.5 we present the ones related to a bivariate setting. Here we compare adjustments $\{\mathbf{t}, \mathbf{c}(\mathbf{t})\} \in \mathcal{A}_K(\alpha_0)$ for various choices of \mathbf{t} . Specifically, we express $\mathbf{t} = t_{\alpha_t, \nu_2} \mathbf{1}_K$ and vary $\alpha_t \in \{0.01, 0.05, 0.1, \dots, 0.45, 0.5\}$. Therefore, the multivariate cTOST $\{\mathbf{0}, \mathbf{c}(\mathbf{0})\}$ defined in (13)-(15) is retrieved at $\alpha_t = 0.5$, and at $\alpha_t = \alpha_0$ we obtain a multivariate extension of the δ -TOST procedure considered in (Boulaguiem et al. 2024). Specifically, fixing $\alpha_0 = 0.05$, $\nu_2 = 20$, and $c_0 = \log(1.25)$, in Figure A.5 we compare the power $\omega_K\{\mathbf{0}, \boldsymbol{\Sigma}_1, \nu_2, \mathbf{t}, \mathbf{c}(\mathbf{t})\}$ of such adjusted procedures (first row), as well as the difference in power with respect to multivariate cTOST, that is, $h(\mathbf{0}, \boldsymbol{\Sigma}_1, \mathbf{0}, \mathbf{t})$ defined in (A.19) (second row). We consider the following settings. (i) Independent setting under heteroskedasticity (first column), where $\rho = 0$, $\sigma_{1,2} = 0.05$ and $\sigma_{1,1}$ increases from 0.05 to 0.2 with a step size of 0.005. (ii) Dependent setting under homoskedasticity (second column), where $\sigma_{1,1} = \sigma_{1,2} = 0.075$ and $\rho \in \{0, 0.05, \dots, 0.9, 0.95, 0.99\}$. (iii) Dependent setting under heteroskedasticity (third column), where $\sigma_{1,1} = 0.125$, $\sigma_{1,2} = 0.075$ and $\rho \in \{0, 0.05, \dots, 0.9, 0.95, 0.99\}$. In all considered scenarios, mul-

tivariate cTOST is always more powerful than other adjusted methods. In all considered scenarios, multivariate cTOST appears to provide superior or comparable power at $\mathbf{0}$, in the sense that, $h(\mathbf{0}, \Sigma_1, \mathbf{0}, t) \geq 0$ after accounting for the simulation error. Indeed, differences in power (second row of Figure A.5) are larger than zero for smaller α_t 's. As α_t approaches the optimal value 0.5, the power gain naturally decreases and the difference eventually shrinks to within simulation error margins (at a 5% significance), represented as gray regions around a power difference of zero, indicated by black dashed lines.

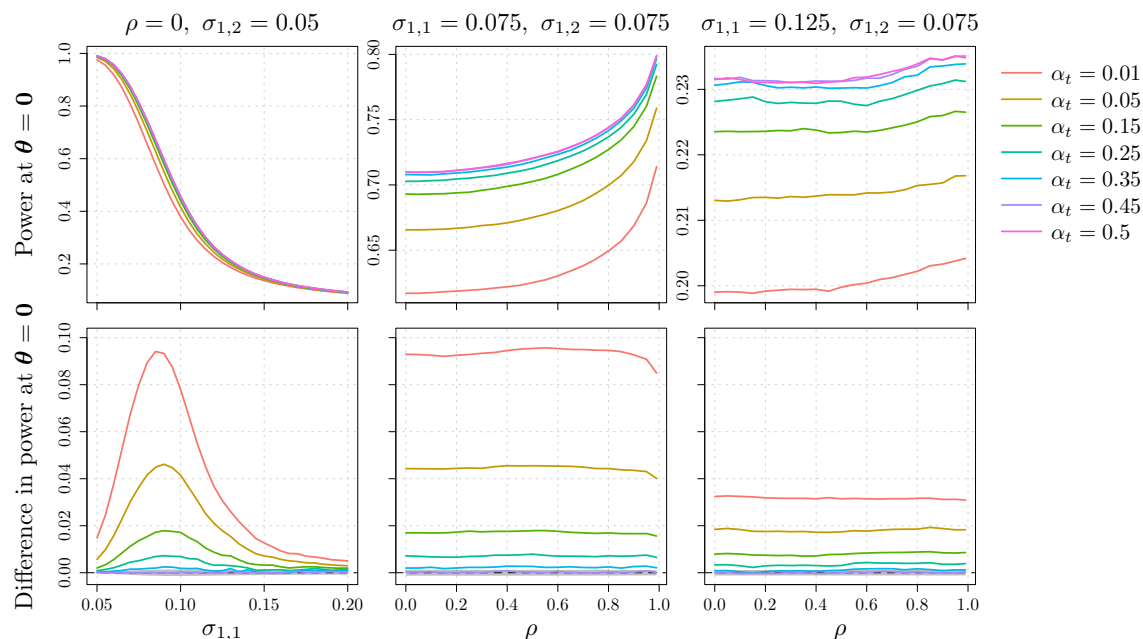


Figure A.5: Comparison of the power at $\theta = \mathbf{0}$ of various multivariate TOST adjusted procedures (first row), and their difference in power with respect to multivariate cTOST (second row), under independence and heteroskedasticity (first column), dependence and homoskedasticity (second column), and dependence and heteroskedasticity (third column).

I Multivariate cTOST versus multivariate α -TOST

It is of interest to highlight the advantages of the proposed multivariate cTOST over the multivariate α -TOST (Boulaguiem et al. 2025), which can be considered as the current state-of-the-art method. The latter arises as a special case of the family of adjustments $\{\mathbf{t}, \mathbf{c}(\mathbf{t})\} \in \mathcal{A}_K^*(\alpha_0)$ in (10) and, therefore, does not generally lead to equal marginal sizes. In particular, similarly to the multivariate TOST, it is obtained when $\mathbf{c} = c_0 \mathbf{1}_K$, but it replaces $t_{\alpha_0} \mathbf{1}_K$ with $t_{\alpha^*} \mathbf{1}_K$, where the same adjusted significance level α^* is employed across all K components to ensure uniqueness and that the resulting adjustment belongs to $\mathcal{A}_K^*(\alpha_0)$. Notably, the operating characteristics of the multivariate α -TOST and the multivariate cTOST are expected to be quite similar under equi-correlation and homoskedasticity (see Section L). However, the multivariate cTOST is preferable when these assumptions are not satisfied, as the multivariate α -TOST adjusts a scalar α^* across all dimensions and thus lacks flexibility. Moreover, the cTOST is computationally much leaner than the multivariate α -TOST, which requires the computation of additional integrals in (9).

The results of the case study in Section 5 highlight the higher flexibility of multivariate cTOST, which effectively leverages information across components by applying greater shrinkage to confidence intervals for dimensions associated with larger variance (where bioequivalence is more difficult to establish) and less shrinkage to dimensions with smaller variance (where it is easier to establish bioequivalence).

Overall, ensuring equal marginal size leads to confidence intervals that remain more comparable across all dimensions.

J Computational details for multivariate cTOST

The algorithm to construct multivariate cTOST adjustments \mathbf{c}^* in (13)-(15) exploits the fact that for a fixed $\boldsymbol{\lambda}(\mathbf{c})$ in (14), one can easily obtain adjustments $\mathbf{c}(\boldsymbol{\lambda})$, by recursively applying Algorithm 1 across each of the K dimensions in \mathbf{c} , where the target significance level α_0 is replaced by $\gamma \geq \alpha_0$ to ensure that all marginal sizes are equal and at the same time the global size remains controlled at α_0 . Specifically, we match the marginal sizes to a γ such that the resulting marginal adjustments $(0, c_k^*) \in \mathcal{A}(\gamma)$, for $k = 1, \dots, K$, lead to the targeted multivariate size $\omega_K\{\boldsymbol{\lambda}(\mathbf{0}, \mathbf{c}^*), \boldsymbol{\Sigma}_1, \nu_2, \mathbf{0}, \mathbf{c}^*\} = \alpha_0$. For a fixed $\boldsymbol{\lambda}(\mathbf{0}, \mathbf{c})$, this algorithm can be shown to converge exponentially fast. However, as $\boldsymbol{\lambda}(\mathbf{0}, \mathbf{c})$ generally depends on the adjustments themselves when $K > 1$, we consider a recursive optimization scheme. Namely, at iteration r , with $r \in \mathbb{N}$, we construct the adjustments

$$\begin{aligned} \mathbf{c}^{(r+1)} &= \underset{\mathbf{c}}{\operatorname{argzero}} \omega_K\{\boldsymbol{\lambda}(\mathbf{0}, \mathbf{c}^{(r)}), \boldsymbol{\Sigma}_1, \nu_2, \mathbf{0}, \mathbf{c}\} - \alpha_0 \\ &\text{s.t. } \omega(c_0, \sigma_{1,1}, \nu_2, 0, c_1) = \dots = \omega(c_0, \sigma_{1,K}, \nu_2, 0, c_K), \end{aligned}$$

where the procedure is initialized at $\mathbf{c}^{(0)} = \mathbf{c}_0$ and iterated until convergence. The formal procedure to compute \mathbf{c}^* is described in Algorithm 2.

Similarly to the univariate framework, we can expect $c_0 > c_k^*$, for all $k = 1, \dots, K$, when σ_1 and K are sufficiently small. Therefore, we can consider the intervals $\widehat{\theta}_k \pm \{c_0 - c_k^*\}$ and, based on the IIP, accept H_1 if all K intervals are entirely contained within the equivalence margins $(-c_0, c_0)$.

Algorithm 2: Algorithm for computing the multivariate cTOST adjustments \mathbf{c}^*

Input : nominal significance level α_0 , equivalence margins c_0 , covariance matrix $\boldsymbol{\Sigma}_1$, degrees of freedom ν_2 , maximum number of iterations r_{\max} , algorithmic tolerance ϵ_{\min} ;

Output: multivariate cTOST adjustments \mathbf{c}^* ;

Set $r = 0$;

Initialize $\mathbf{c}^{(0)} = \mathbf{c}_0$;

Obtain $\boldsymbol{\lambda}\{\mathbf{c}^{(0)}\}$ as in (14);

while $|\omega_K[\boldsymbol{\lambda}\{\mathbf{c}^{(r)}\}, \boldsymbol{\Sigma}_1, \nu_2, \mathbf{0}, \mathbf{c}^{(r)}] - \alpha_0| > \epsilon_{\min}$ and $r \leq r_{\max}$ **do**

 Initialize $\gamma^{(0)} = \alpha_0$;

 Obtain $\mathbf{c}^{(r,0)}$ with Algorithm 1 where $\{0, c_k^{(r,0)}\} \in \mathcal{A}(\gamma^{(0)})$, for $k = 1, \dots, K$;

 Obtain $\gamma^{(1)} = \gamma^{(0)} + \alpha_0 - \omega_K[\boldsymbol{\lambda}\{\mathbf{c}^{(r)}\}, \boldsymbol{\Sigma}_1, \nu_2, \mathbf{0}, \mathbf{c}^{(r,0)}]$;

 Initialize $u = 0$;

while $|\gamma^{(u+1)} - \gamma^{(u)}| > \epsilon_{\min}$ **do**

 Set $u = u + 1$;

 Obtain $\gamma^{(u+1)} = \gamma^{(u)} + \alpha_0 - \omega_K[\boldsymbol{\lambda}\{\mathbf{c}^{(r)}\}, \boldsymbol{\Sigma}_1, \nu_2, \mathbf{0}, \mathbf{c}^{(r,u)}]$;

 Obtain $\mathbf{c}^{(r,u+1)}$ with Algorithm 1, where $\{0, c_k^{(r,u+1)}\} \in \mathcal{A}(\gamma^{(u+1)})$, for $k = 1, \dots, K$;

end

 Set $r = r + 1$;

 Store the adjustment $\mathbf{c}^{(r)} = \mathbf{c}^{(r,u)}$;

 Compute $\boldsymbol{\lambda}\{\mathbf{c}^{(r)}\}$ in (14);

end

Output the multivariate cTOST adjustment $\mathbf{c}^* = \mathbf{c}^{(r)}$

K Extended univariate simulation results

In this section, we present the results of a more extensive simulation study for the univariate setting presented in Section 4.1.

K.1 Setting 1

We first consider the canonical form defined in (2) for $K = 1$, where 34 equally-spaced values from the interval $[0, 0.26]$ are considered for θ , including the value of $c_0 = \log(1.25)$ which provides the value at which we compute the size of any given method as defined in (4). For the standard error of $\hat{\theta}$ we consider $\sigma_1 \in \{0.08, 0.12, 0.16\}$, and vary the degrees of freedom $\nu_2 \in \{5, 10, 15, 20, 30, 40\}$. All tests are conducted at the nominal significance level $\alpha_0 = 5\%$, based on 10^5 Monte Carlo samples.

Figure A.6 compares the probability of rejecting H_0 as a function of θ for the TOST, α -TOST, cTOST and cTOST*, where $\nu_2 \in \{5, 10, 15\}$. Here cTOST* consistently achieves an empirical size closest to the nominal level α_0 while simultaneously demonstrating uniformly greater power than the TOST and α -TOST. While cTOST is most powerful across all simulation settings, it leads to a slightly liberal test procedure for smaller sample sizes ($\nu_2 < 15$). Similar results hold for settings with larger degrees of freedom $\nu_2 \in \{20, 30, 40\}$ as shown in Figure A.7.

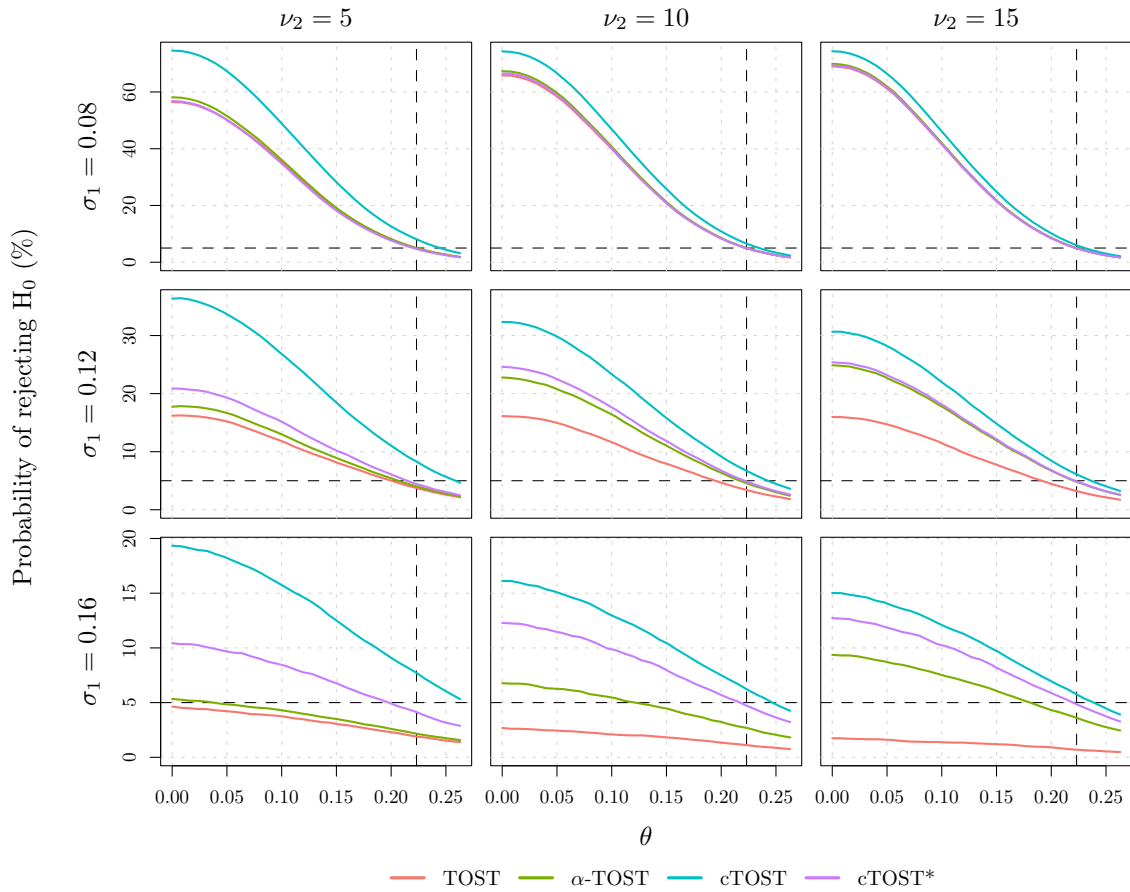


Figure A.6: Probability of rejecting the null hypothesis as a function of θ , for the TOST, α -TOST, cTOST and cTOST*, across different degrees of freedom ν_2 (columns) and standard errors (rows).

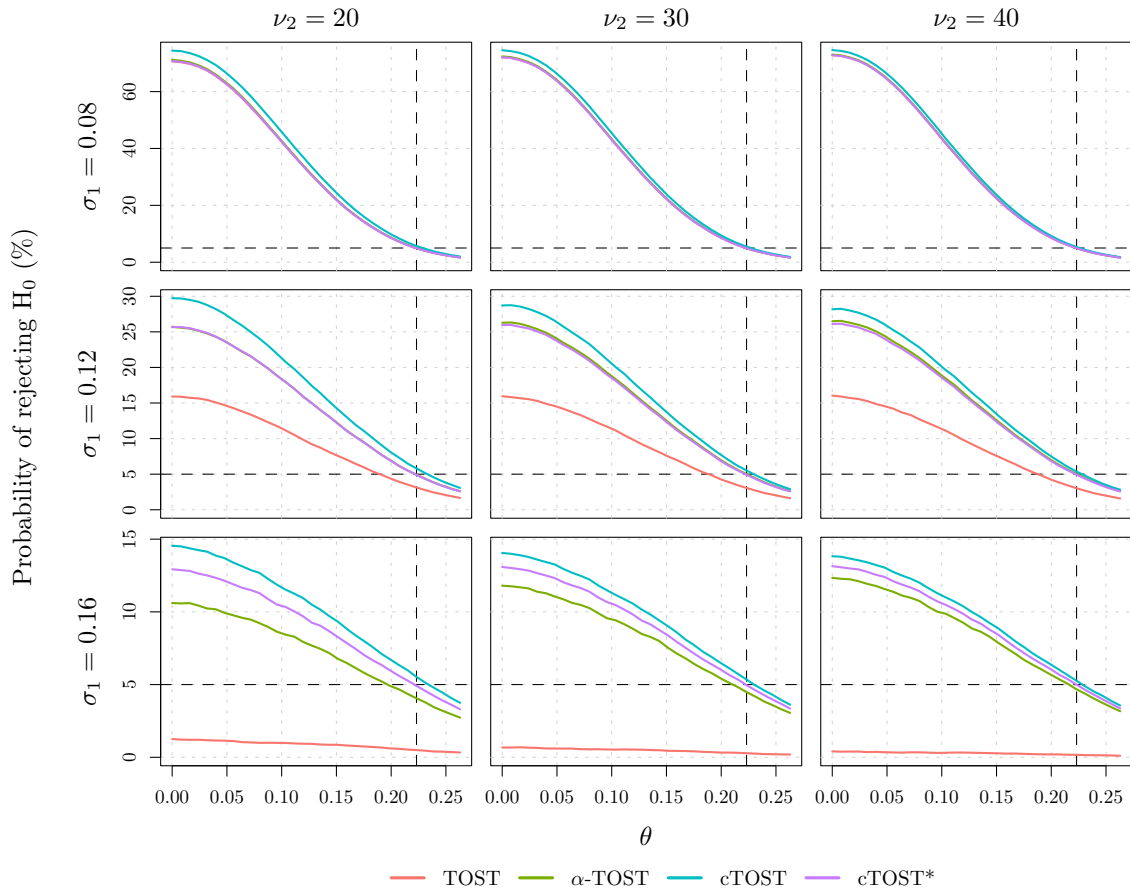


Figure A.7: Probability of rejecting the null hypothesis as a function of θ , for the TOST, α -TOST, cTOST and cTOST*, across different degrees of freedom ν_2 (columns) and standard errors (rows).

K.2 Setting 2

Next, we compare the empirical size of various test procedures across a variety of settings. We set $c_0 = \log(1.25)$, $\alpha_0 = 5\%$, and increase σ_1 from 0.01 to 0.3 with a step size of 0.005, and ν_2 from 20 to 80 with a step size of 1. To evaluate the empirical test size, we fix $\theta = c_0$. Figures A.8-A.11 show simulation results respectively for TOST, α -TOST, cTOST and cTOST*. Across all simulation scenarios, while cTOST has a slightly liberal size for smaller ν_2 's and σ_1 's, cTOST* consistently maintains a size closest to the nominal level α_0 . In contrast, both TOST and α -TOST procedures often lead to conservative tests.

This pattern is further illustrated in Figure A.12, which reports the empirical test size across these simulation scenarios. The cTOST* procedure yields a test size that typically remains within the simulation error tolerance (displayed as a gray region around $\alpha_0 = 5\%$). On the other hand, cTOST occasionally demonstrates liberal behavior. While TOST shows extreme conservativeness, with 33% of the occurrences leading to a size of zero, α -TOST moderately improves upon this limitation but remains substantially conservative. Finally, Figure A.13 illustrates the difference in power at $\theta = 0$ relative to the α -TOST. These results confirm that cTOST achieves superior power performance. Although cTOST* leads to slightly reduced power compared to cTOST as a trade-off for more precise size control, it typically outperforms both TOST and α -TOST procedures in terms of statistical power.

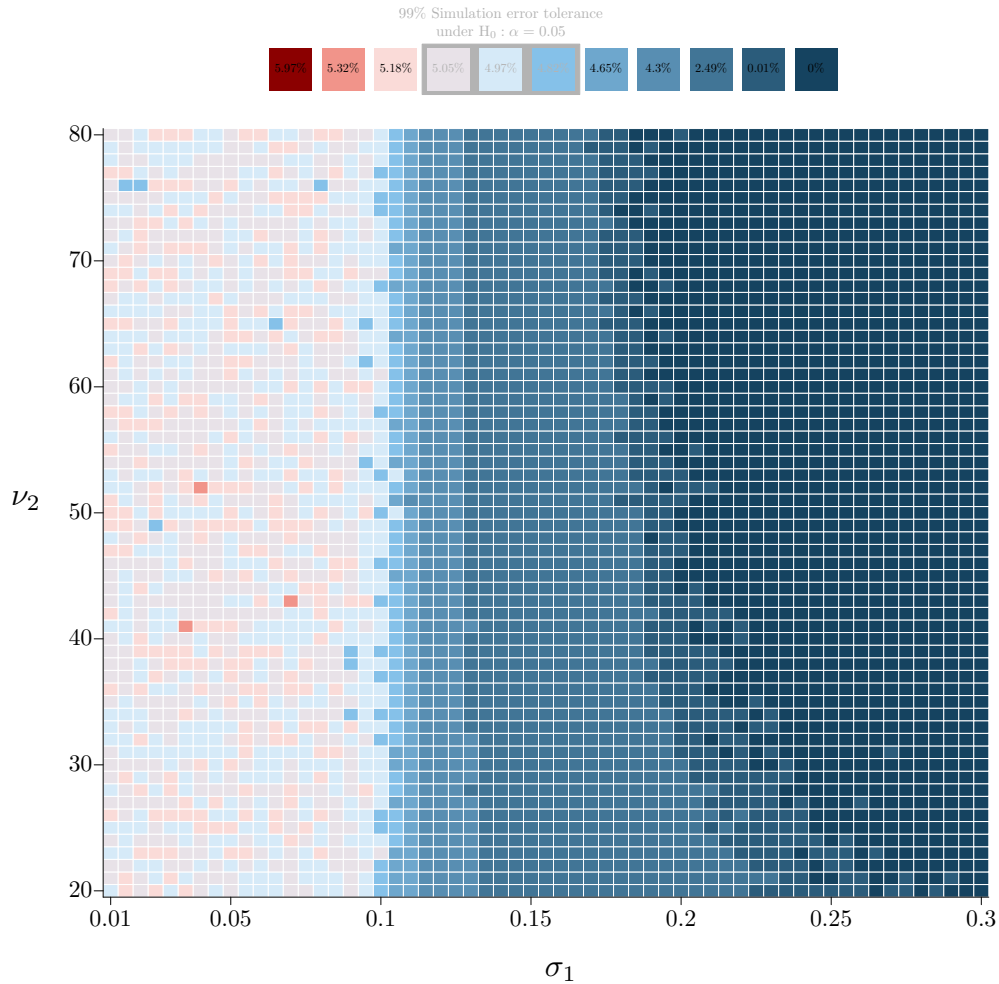


Figure A.8: Heatmap representing the empirical size (in %) of the TOST (color gradient) as a function of σ_1 (x -axis) and ν_2 (y -axis). The lighter colors, highlighted in gray in the legend, correspond to the $\alpha_0 = 5\%$ nominal level, up to a simulation error. This error was assessed by a two-sided binomial exact test at the 1% level, based on results from 10^5 Monte Carlo samples per setting.

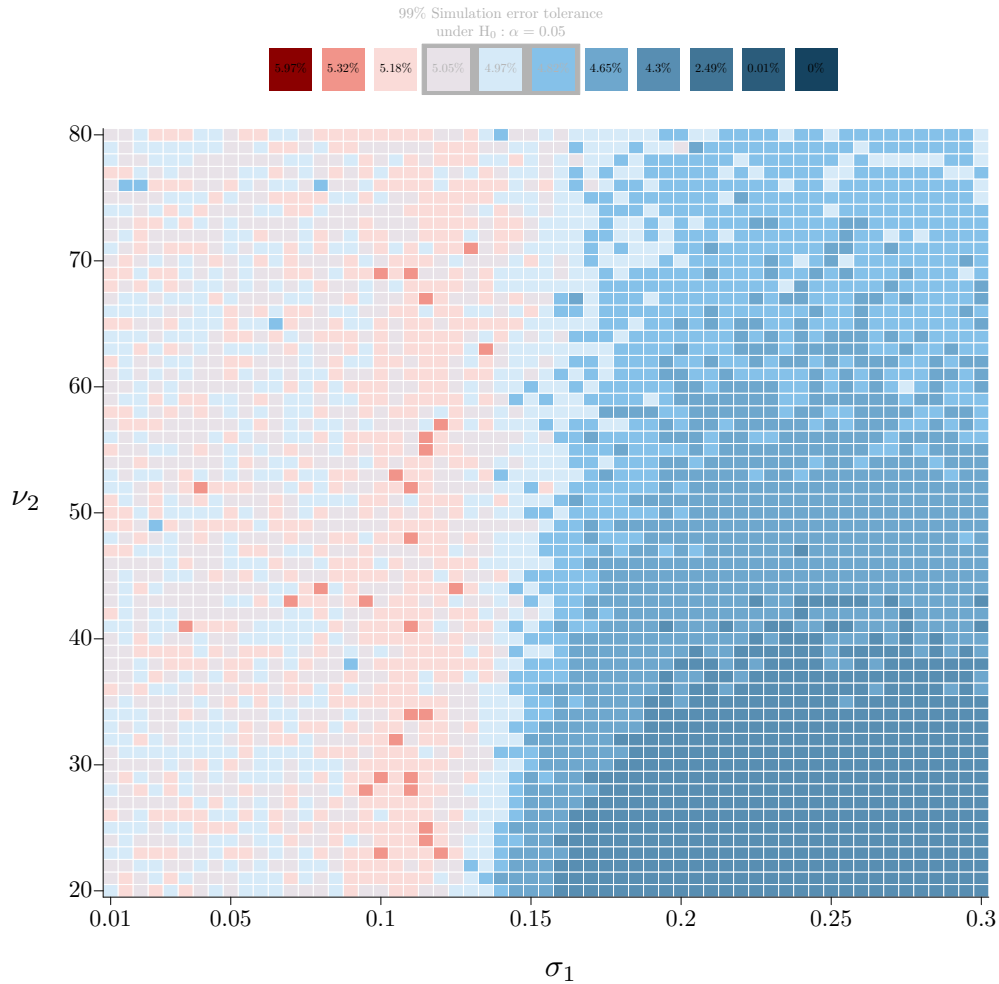


Figure A.9: Heatmap representing the empirical size (in %) of the α -TOST (color gradient) as a function of σ_1 (x -axis) and ν_2 (y -axis). The lighter colors, highlighted in gray in the legend, correspond to the $\alpha_0 = 5\%$ nominal level, up to a simulation error. This error was assessed by a two-sided binomial exact test at the 1% level, based on results from 10^5 Monte Carlo samples per setting.

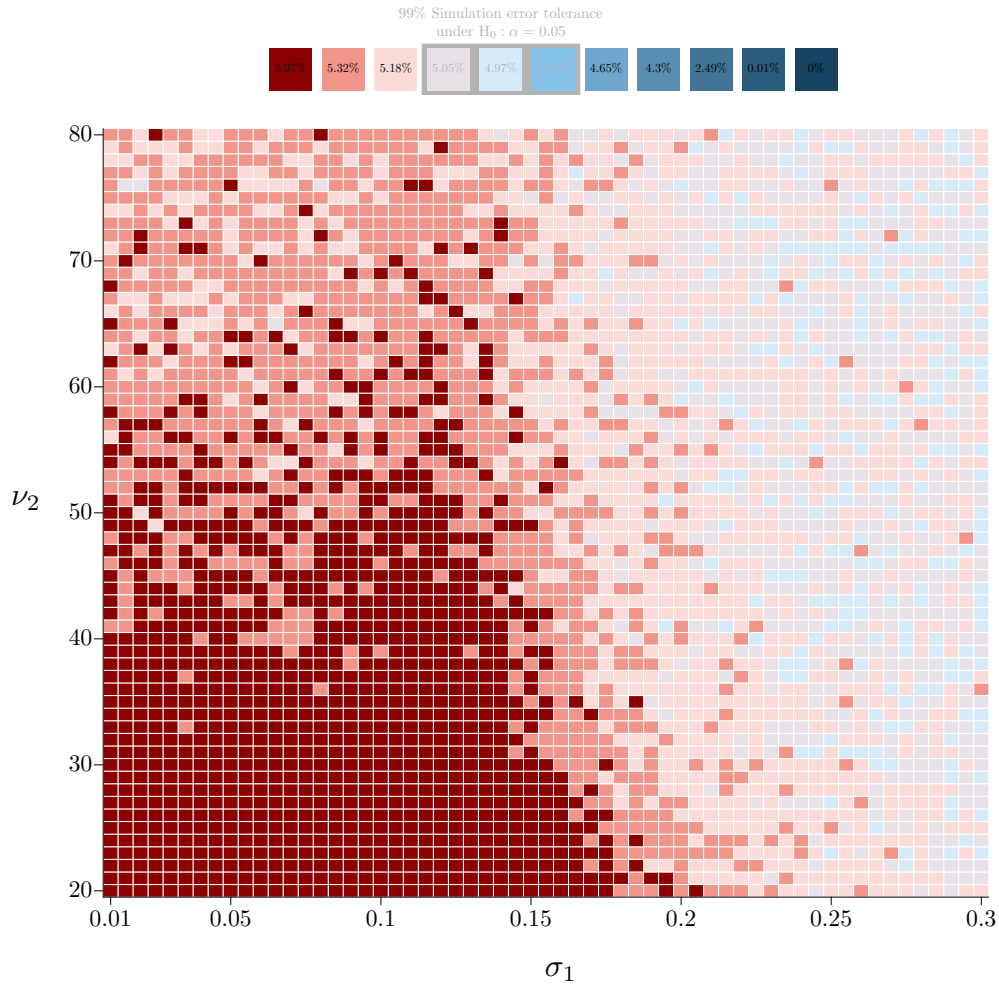


Figure A.10: Heatmap representing the empirical size (in %) of the cTOST (color gradient) as a function of σ_1 (x -axis) and ν_2 (y -axis). The lighter colors, highlighted in gray in the legend, correspond to the $\alpha_0 = 5\%$ nominal level, up to a simulation error. This error was assessed by a two-sided binomial exact test at the 1% level, based on results from 10^5 Monte Carlo samples per setting.

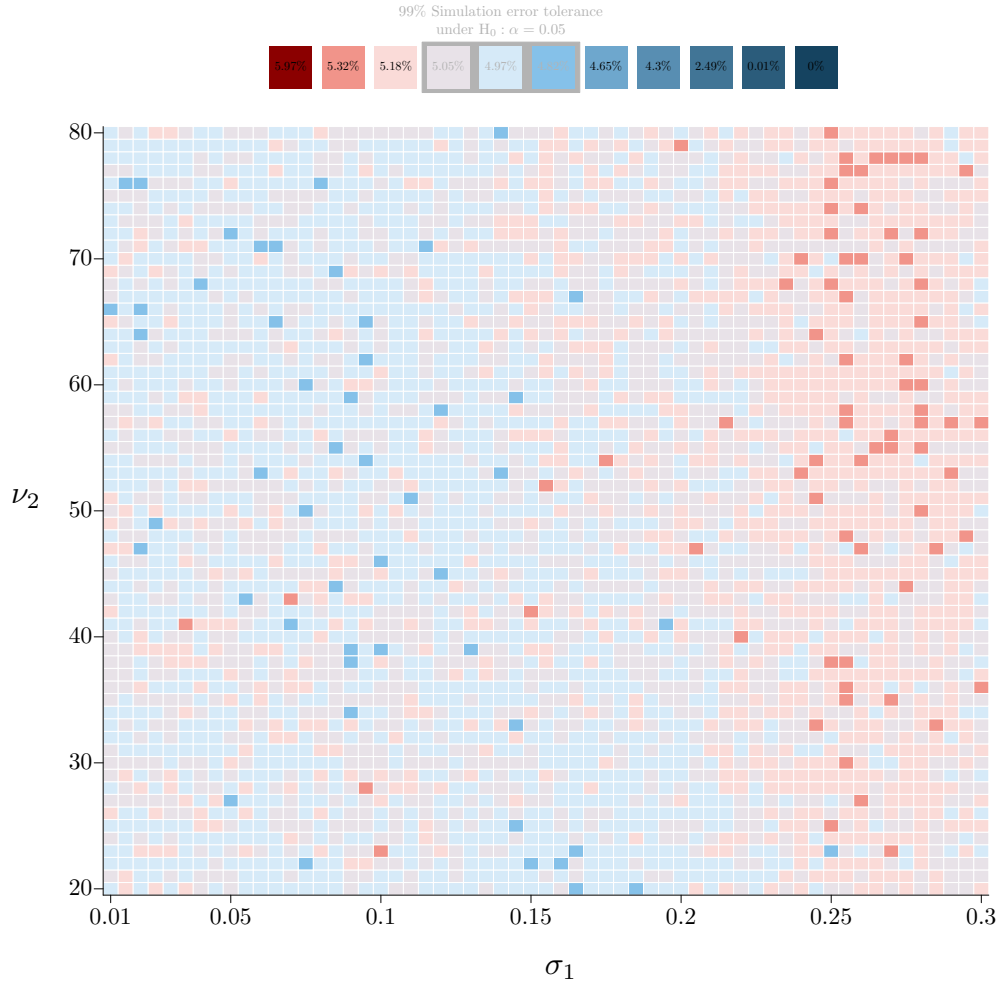


Figure A.11: Heatmap representing the empirical size (in %) of the $cTOST^*$ (color gradient) as a function of σ_1 (x -axis) and ν_2 (y -axis). The lighter colors, highlighted in gray in the legend, correspond to the $\alpha_0 = 5\%$ nominal level, up to a simulation error. This error was assessed by a two-sided binomial exact test at the 1% level, based on results from 10^5 Monte Carlo samples per setting.

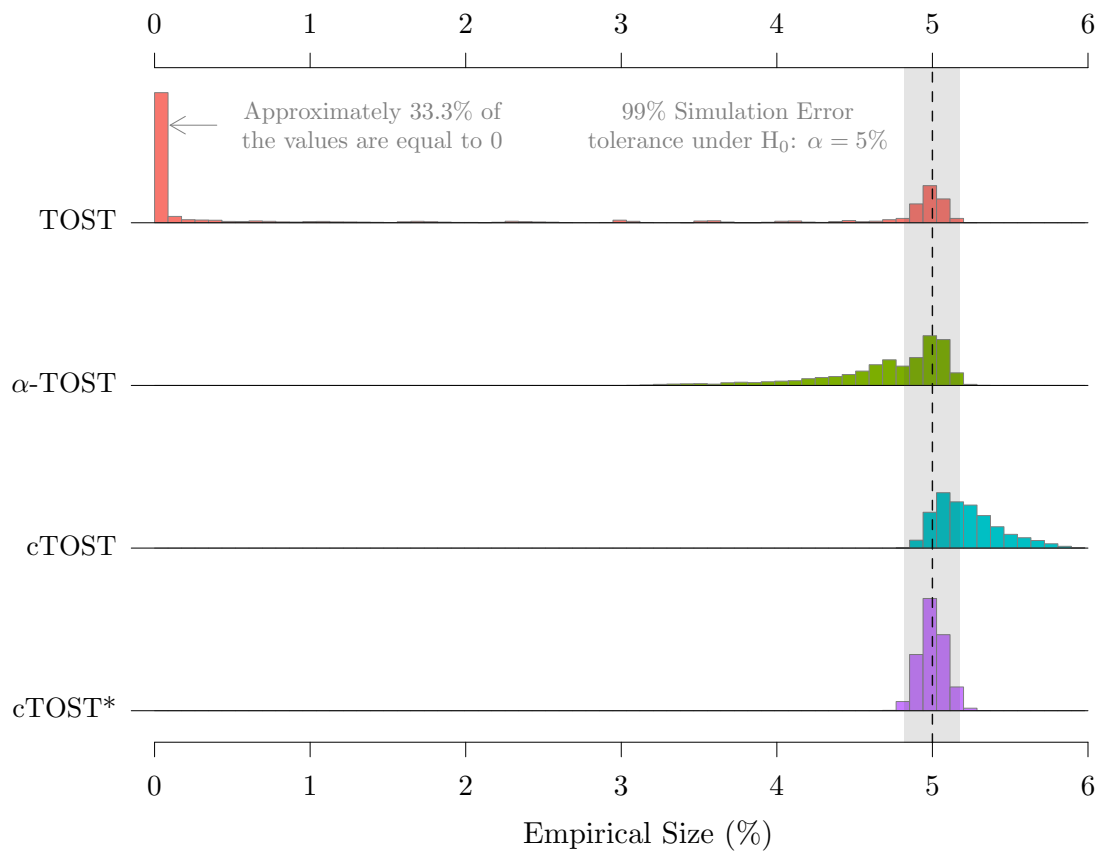


Figure A.12: Histograms reporting the empirical test size of TOST, α -TOST, cTOST and cTOST* when varying σ_1 and ν_2 .

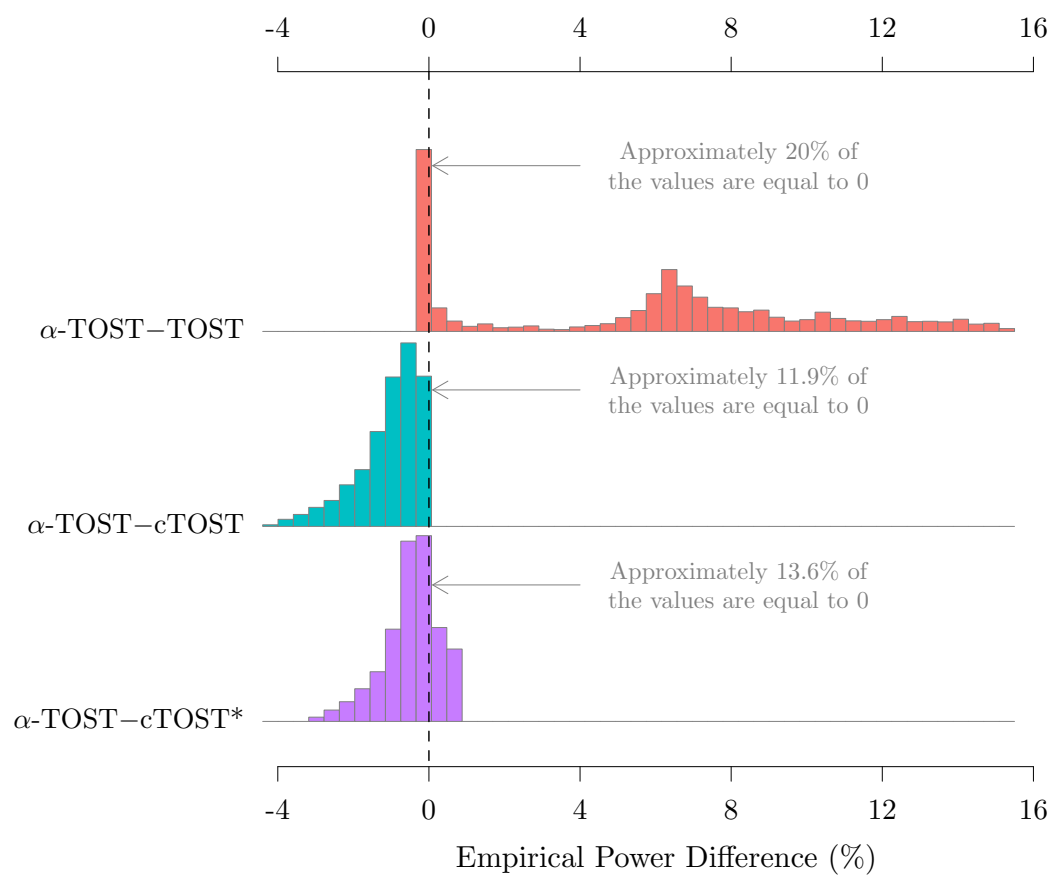


Figure A.13: Histograms reporting the difference in power at $\theta = 0$ for TOST, cTOST and cTOST* relative to α -TOST when varying σ_1 and ν_2 .

L Extended multivariate simulation results

For the multivariate simulation settings of Section 4.2, Figure A.14 compares the performance of multivariate TOST, α -TOST and cTOST. Across all scenarios, the multivariate cTOST outperforms multivariate α -TOST in terms of power, while more accurately controlling the test size at the nominal level.

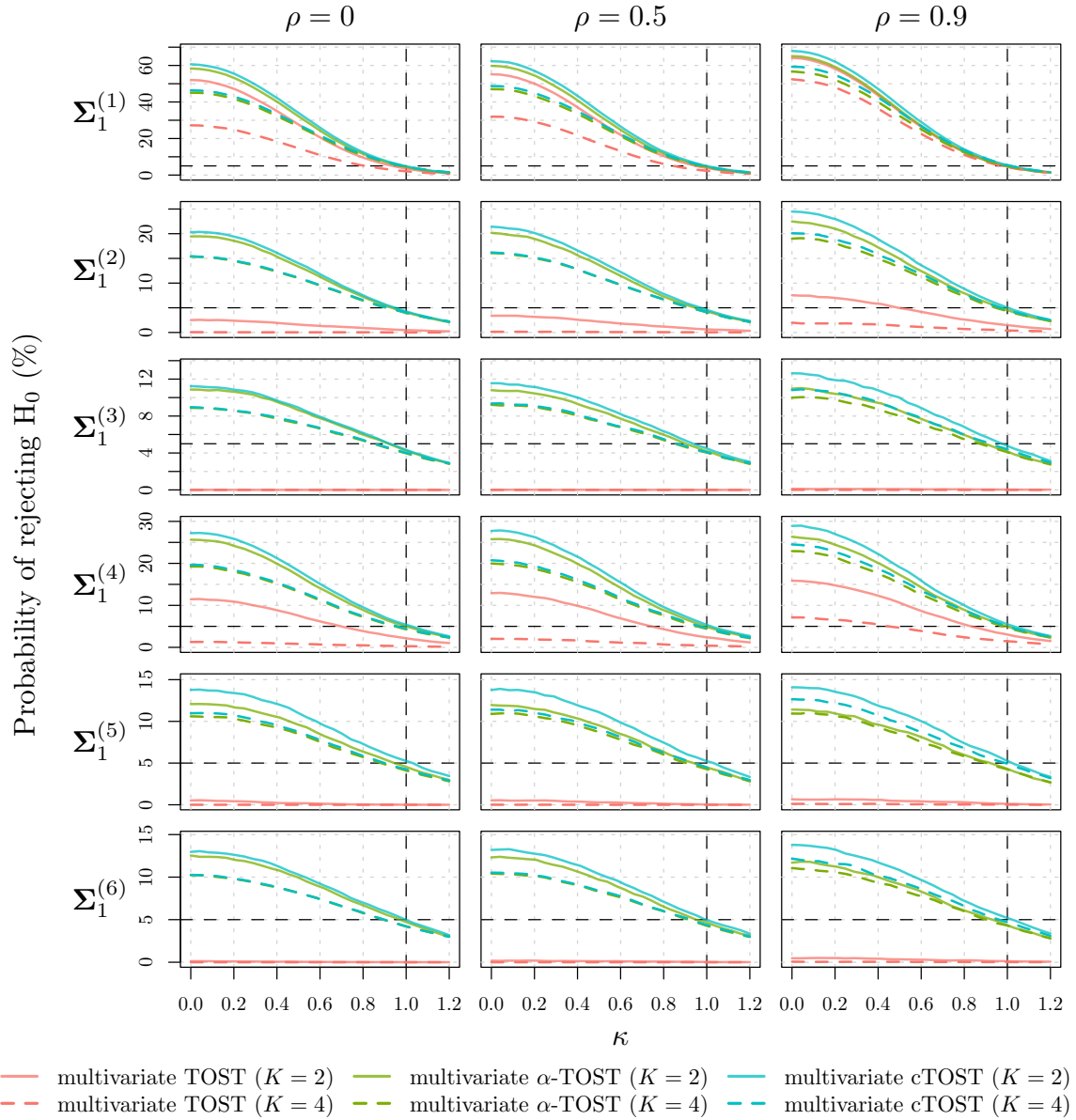


Figure A.14: Probability of rejecting the null hypothesis as a function of κ , for the multivariate TOST, the multivariate α -TOST, and the multivariate cTOST across different levels of correlation ρ (columns) and covariance matrices (rows), for the bivariate (solid lines) and 4-variate (dashed lines) settings.